# UNIVERSITY OF READING

Department of Meteorology

Impact of future climate change on extreme rainfall events in Oman

Sara Khatab

MSc. Applied Meteorology and Climate with Management

August 2018

Abstract

The occurrence of extreme rainfall events and flash floods in many areas during recent years is a motivation to study long-term changes in extreme rainfall over Oman. The risk from the possible impacts of climate change has been growing with the recent cyclones that had affected the country. Gas and oil companies like British Petroleum (BP) require a deep knowledge about the past, the present climate and require an accurate estimation of the plausible change in extreme rainfall events.

This dissertation project looks at the impact of climate change on daily extreme rainfall events in desert environments given as an example the Sultanate of Oman. The study presents a rather complete picture about the current (1999-2005) and future (2035-2065) projection of the daily extreme rainfall events and the spatial distribution of rainfall over Oman. The analysis for the present period is done for daily precipitation using 12 station data, gridded data (GPCP), and CMIP 5 models considering scenario RCP 4.5. The empirical quantile method is used as a bias correction method for AMIP, Historical simulations, and projections in comparison to the GPCP data, that gave satisfactory results.

The results showed that gridded (GPCP) data can capture some daily extreme events like the station data but usually underestimates the magnitude of the events. The models indicate that there will be an increase in the daily extreme events in southern Oman, a decrease in northern Oman, and a slight decrease in the interior region. There is an increase in the mean relative precipitation in northern Oman, (-5 to 5%), (5 to 10%) in the interior region, and (10 to 15%) in southern Oman, relative to the present day.

Keywords: extreme rainfall, climate change, quantile mapping, gridded data, RCP 4.5 scenario

Acknowledgments

Contents

1 Introduction

Rainfall plays an important role in the climate system and it is essential to life on land, as it is a source of water for drinking and supporting crops. Recent changes in daily or even hourly precipitation events are of great interest due to possible significant hydrological effects such as flash floods (Ban et al., 2015). Thermodynamics can help to evaluate potential future changes in precipitation extremes. To be more precise, in the atmosphere the saturation water vapour pressure is a function of temperature which according to the Clausius-Clapeyron equation, increases at a rate of 6-7% per degree of surface warming (Ban et al., 2015). Studies suggest that due to energy limitations, extreme precipitation events may increase at this rate, however, mean global precipitation increases at a slower rate of 1-3% per degree (O'Gorman and Schneider, 2008). The IPCC report shows many regions of decreasing total precipitation but increasing 5-day maximum intensity extremes. It is worth mentioning that an extreme in one region may not be extreme in another (Pendergrass et al., 2018).

This study is focusing on dry environments where heavy rain is uncommon but can have substantial impact (Al-Awadhi et al., 2018). Research has shown that extreme events that used to be rare 50 years ago are recently becoming frequent in most parts of the world due to climate change (Alexander et al., 2006). Alexander et al. (2006) examined different climate indices derived from daily precipitation and daily temperature, with a focus on extremes. They used an exact formula and a specific software that allowed a satisfying and comprehensive global picture of the trends. Pianka (1970), Slobodkin and Sanders (1969) argued that desert precipitation is more variable than that of other environments and is often defined as "unpredictable". Based on projections made by global circulation models and regional climate models, Fowler et al. (2005) and Beniston et al. (2007) argue that anthropogenic climate change can lead to an increase in the frequency of extreme weather events. This suggests that extreme rainfall events may become more frequent in the upcoming decades. On the other hand, internal variability of the climate system may cause changes in atmospheric circulation that contribute to or counteract these effects (Allen and Ingram, 2002). Hence, understanding the occurrence of past rainfall extremes can avoid or at least reduce future disaster.

This study will use as an example of a dry environment the Sultanate of Oman, which is in the Arabian Peninsula. According to Al Rawas (2009) and MRMEWR (2015), Oman witnessed 10 major flash floods from 1989 to 2014. The most recent, strongest cyclone on record in the

Arabian Sea, hurricane Mekunu on the 25th of May 2018, led to major flash flooding in Oman, with the total rainfall reaching 617 mm near the coast of Salalah that caused 7 deaths. (Times of Oman, 2018). Arid and semi-arid regions like Oman, encounter catastrophic flash floods, long periods of droughts and chronic water stress (Gunawardhana and Al-Rawas, 2014). Oman has been facing lately increased frequency of flooding, mostly flash floods (Al-Rawas and Valeo, 2010).

In the past, oil and gas production facilities have been designed using historical weather to capture the extremes in an environment. While this has previously proved practical, the world's changing climate means that this method may no longer provide a realistic evaluation of the conditions that the facilities will have to operate in, in the coming years and decades. This has implications for facilities efficiency, longevity and workforce safety and therefore, commercial viability.

The industrial partner for this project, BP, is a British global oil and gas company based in London. They are interested in the impact of climate change on extreme rainfall and flash flooding in the desert environments where they construct major projects. To be more precise, BP is currently working on a project under construction in the south of Block 61 in the Ad Dhahirah Governorate of Oman. It is called Khazzan Phase 2 (Ghazeer), and it is expected to be complete by 2021. The second phase of the onshore Khazzan field development involves drilling approximately 100 wells, construction of a third trainline, a new export pipeline and tie-in to the existing Phase 1 facilities. The second phase (Ghazeer) is expected to deliver an additional 0.5 billion cubic feet per day (bcf/d) and over 15.000 barrels a day of condensate, bringing total Khazzan gas production to approximately 1.5bcf/d (Bp.com, 2016). Hence, it is of major importance for the company to understand the risk posed by extreme rainfall events and flash flooding in this area, that could affect their project.

The most recent study that has been conducted for flood risk assessment in Muscat, Oman was undertaken by Al-Awadhi et al. (2018). The study coupled flooding hazard maps with land use cover using GIS and they identified areas with high, medium, and low-risk exposure from extreme rainfall events that could lead to disaster. Such research reinforces the importance of flood risk management and mitigation and the danger imposed by extreme rainfall. Al-Sharmi et al. (2011) studied the recent climate change observed over the Arabian Peninsula and over Oman. They used 8 stations covering the period 1980-2013. Only two of the stations showed negative trends in annual rainfall accumulation (Saiq: −74.0 mm/decade and Salalah: −10.8

mm/decade), while the rest of the stations showed negative but not significant trends. On the contrary, Salalah is in the southwestern part of Oman where according to Al Charaabi et al. (2013), the area is expected to receive more annual rainfall at a rate of 20 to 40 mm by 2040.

Al-Kalbani et al. (2015) examined the recent trends in temperature and precipitation in a mountainous area called Al Jabal Al Akhdar, Oman, and the implications for future climate change. The original aspect of this study is that, to the knowledge of this author, it is the first in such a region. They found out that for the record 1979-2012, there is a decrease in precipitation (-9.42 mm/decade), which coincides with the projections made for northern Oman where precipitation will decrease by 2040 (Al Charaabi and Al-Yahyai, 2013). A similar study has been done by Al-Rawas et al. (2015), where they investigated how climate change affects the magnitude and occurrence of extreme precipitation and the impact it has on the wadi flow regime in the Al-Khod catchment area, Muscat, Oman. They used six-member ensembles of Global Climate Models (GCMs) from the Coupled Model Intercomparison Project 5 (CMIP5), and the result indicated that there is a constant increase in extreme precipitation for all return periods by the middle of the 21st century (49-52%), relative to the present day. According to their study, they class as annual rainfall extreme above 75 mm. They also concluded that changes are expected to increase even more by the end of the century (81-101%).

Trends in extreme temperature and precipitation in Muscat, Oman were analysed by Gunawardhana and Al-Rawas (2014). They used daily data for precipitation over the period 1977-2011 and a set of climate indices. The results showed a shift towards wetter conditions with a rate of 6 mm annual precipitation per decade, which can be attributed to the increase of extreme rainfall events. Al Charaabi and Al-Yahyai (2013) looked at the projection of future changes in temperature and rainfall in Oman. They used the Fourth Assessment Report AR4 A1B forcing scenario, that assumes a balance in all energy sources, with the climate model of NCAR and the CCSM-3. The study concluded that northern Oman is expected to encounter decreasing rainfall in the next decades. It is expected that climate change will lead to a decrease of 20 to 40 mm annual rainfall by 2040, which is equivalent to a 40% reduction in the average annual rainfall of Oman.

Kwarteng et al. (2008) analysed rainfall data for the period 1977 to 2003 in the Sultanate of Oman. They used Mann-Kendall statistics which showed a negative but significant trend for the datasets. Their research is of major importance as it indicates the rainfall intensity that is associated to flash floods in Oman, which is rainfall above 50 mm/day. This threshold will be

used as a reference in this study for the station data used. The records also showed that Muscat and the cities surrounding are vulnerable to tropical cyclones and disastrous rainfall (above 100 mm/day), almost every 50 years. Goswami et al. (2006) examined the trend of extreme rainfall over India using gridded data for the period 1951-2003. They concluded that there is an increase in the frequency and magnitude of extreme rainfall events, and a decreasing frequency in moderate events over central India. It is worth mentioning that even though gridded data have good quality control and spatial coverage than station data, gridded data cannot capture most of the time the local extreme events, they usually capture large-scale events. This happens due to the interpolation or averaging method used in gridding (Metoffice.gov.uk, 2018). Using only gridded data for analysis of extreme events can be misleading when it comes to disaster management, so it is better to use station data for such research (Guhathakurta et al., 2011).

This dissertation project looks at the impact of climate change on extreme rainfall events in desert environments given as an example the Sultanate of Oman. To obtain a clear idea of the impact of climate change on extreme rainfall events, a thorough study of extreme rainfall events in dry environments like Oman is required using the latest data available. It is worth mentioning that understanding the changes in extremes is more crucial than the changes in mean pattern, for better disaster management (Guhathakurta et al., 2011). Based on the above, the objectives of the present work are:

- To study what rainfall intensity/duration is linked to flash flooding in Oman.
- How often such events occur in the daily station data.
- What synoptic conditions lead to these rainfall events.
- To check whether gridded (1 degree) daily precipitation data represent extreme events.
- To evaluate how well climate model simulations, represent the spatial/temporal/intensity rainfall distribution.
- To examine how heavy rainfall changes in the future.

The balance of this dissertation is organised as follows:

Chapter 2 includes an overview of the topography, climatology and the rainfall mechanisms over Oman.

Chapter 3 includes the methodology followed and the data used. Observations are described and the uncertainty, as well as the models and the main methods that are used throughout.

Chapter 4 includes the observed characteristics of extreme events, where station data and gridded data are analysed. Events are identified as case studies and their synoptic precursors.

Chapter 5 simulated extremes are evaluated by comparing AMIP and Historical model simulations. Bias correction is proposed to make simulations represent observed extremes.

Chapter 6 includes the climate change projections for Oman.

Chapter 7 is the last chapter with the conclusions.

2 An overview of the topography, climatology and rainfall mechanisms over Oman

2.1 Topography and climatology of Oman

The Sultanate of Oman is in the south-eastern part of the Arabian Peninsula. It is extended between latitude 23° 36' 51" N, longitude 58° 32' 43" E, and it occupies an area of approximately 312.500 km^2 (Latlong.com, 2018). It neighbours Yemen in the southeast, the United Arab Emirates (UAE) in the northwest, and the Kingdom of Saudi Arabia (KSA) in the west.

As seen in *Figure 1*, Oman covers a distinct range of topography that includes arid deserts, mountain ranges, and fruitful plains (Gunawardhana et al., 2015). The area can be divided into three topographic regions (Kwarteng et al., 2009):

- The interior region that consists of a sandy desert, and it is in the area between the mountain ranges in the north and south. It also accounts for 82% of Oman, with elevations that do not exceed 500 m.

- Mountain ranges like Al Hajar Mountains, and Qara Mountains in the north that occupy 15% of the country. There are also known for the northern Oman mountains and they extend around 700 km and the highest peak reaches approximately 3075 m above sea level. In southwestern Oman, the Dhofar mountains can be found, and they reach approximately 2000 m above sea level.

- Coastal plains that account for 3% of the country and extend from the north in Batinah to the south in Salalah. These areas are mainly agricultural, and the elevations range from 0 to 500 m.
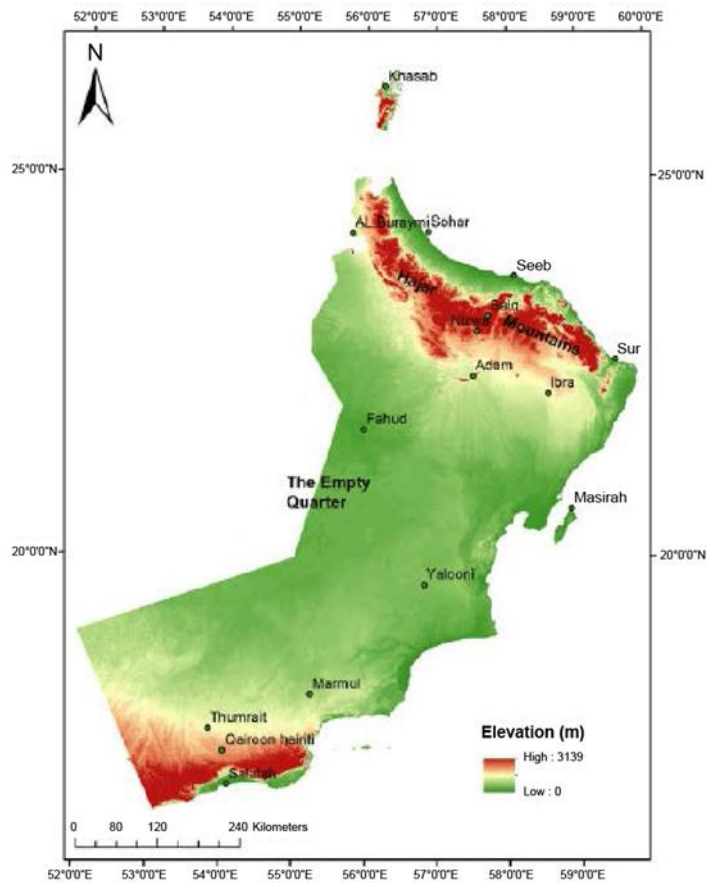
Figure 1: Topography of Oman. Source: (Al Charaabi and Al-Yahyai, 2013).
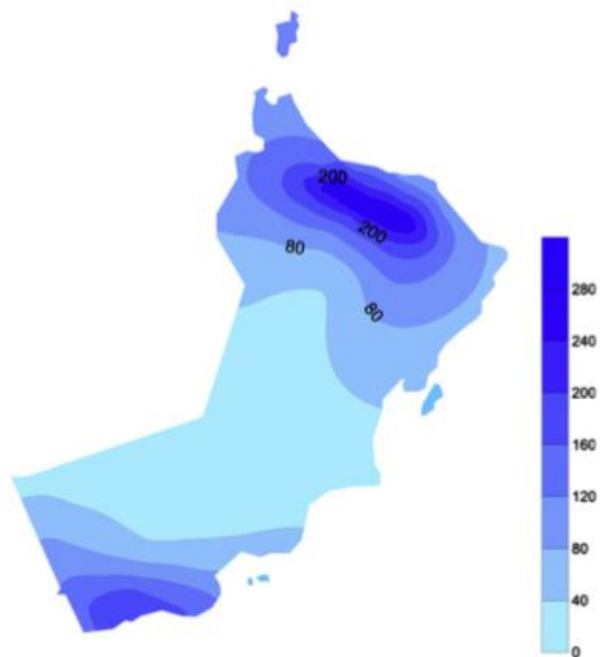
Figure 2: Spatial annual rainfall variability over Oman relative to 1984-2007. Source: (Charabi and Al-Hatrushi, 2010).

The distinct topography of Oman influences the precipitation patterns (Kwarteng et al., 2009; Gunawardhana et al., 2015). The average temperature in northern Oman ranges from 32 to 36ºC depending on the season. While in the interior section of Oman, temperatures extend from 15 to 50ºC depending again on the season, but the coastal regions usually reach 46ºC and high levels of humidity (Kwarteng et al., 2009). Precipitation in Oman is irregular, low, and infrequent over much of the country (see *Figure 2*), which also indicates spatial variability (Gunawardhana et al., 2015). That means that over the mountainous regions, the mean annual precipitation reaches 350 mm, however, in the coastal regions it is less than 100 mm (Gunawardhanaet al., 2015). During the period 1977 to 2011, the contribution of very wet days to the total precipitation increased, which is highly associated with increases of extreme precipitation in recent decades (Gunawardhana and Al-Rawas, 2014).

2.2 Rainfall mechanisms over Oman

The diverse topography of Oman along with other meteorological conditions result in rainfall variability across the country. There are four principal synoptic atmospheric mechanisms that cause rainfall over Oman (Al Charaabi and Al-Yahyai, 2013):

- During summer from June to September, the southern coast of Oman is affected by the Tropical Maritime air mass (see *Figure 2*), and Indian Monsoon circulation bringing rainfall to the Dhofar Mountains. The area is also affected by cyclones approximately every five years. In northern Oman, local orographic convection is formed bringing heavy rainfall to the Hajar Mountain range during summer. This is mainly caused by the sea breeze circulations. (Al-Hatrushi, 2012; Kwarteng et al., 2008).

- During winter from December to February, northern Oman is exposed to the Polar Maritime and Polar Continental air masses, that bring moisture from the Mediterranean Sea and the North Atlantic respectively. This moisture is favoured by the low-pressure systems and the moving upper troughs (Kwarteng et al., 2008).

- During spring from March to May, the Tropical Continental air mass meets the Polar Continental air mass. This causes heavy rainfall in the Dhofar Governorate, especially at Fahud where 60% of its annual rainfall falls during this period. The same happens to Masirah Island where 50% of the rainfall falls during this period as well (Charabi and Al-Hatrushi, 2010).
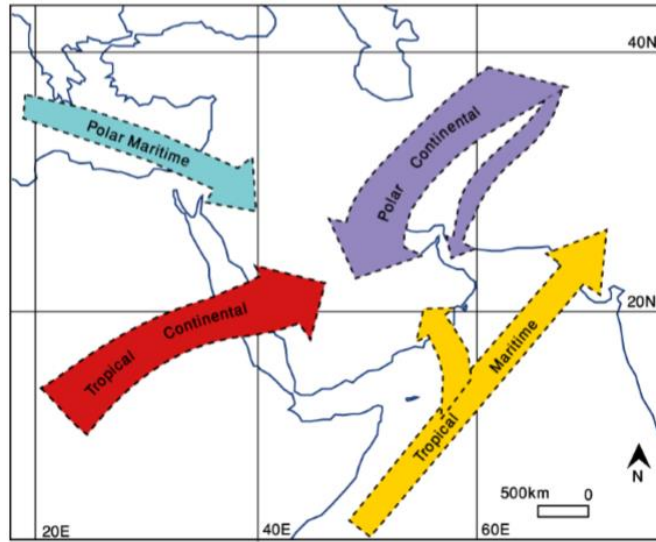
Figure 3: Air masses affecting the climate over Oman. Source: (Al-Hatrushi, 2012).

3 Data Sets and Methodology

3.1 Data Sets

3.1.1 Station rain gauge observations

Daily accumulated total rainfall data in 28 rain gauge stations were considered initially, but only 12 were used (see *Figure 3*). The reason was that most of the stations had records less than 30 years, which was not used for a climatological analysis. The GHCN-D v2 daily station data (Global Historical Climatology Network) are for a period between 1983-2018 and were downloaded from KNMI Climate Explorer. To be more precise, the GHCN-D dataset from NCDC/NOAA collects data from around the world, however, the coverage is not that even as some countries refuse to share daily data. The data are obtained from two sources: from the weather services and the GTS (Global Telecommunication System), which brings the records up to date but can be inaccurate with missing data and misplaced decimal points (Ncdc.noaa.gov, 2018).
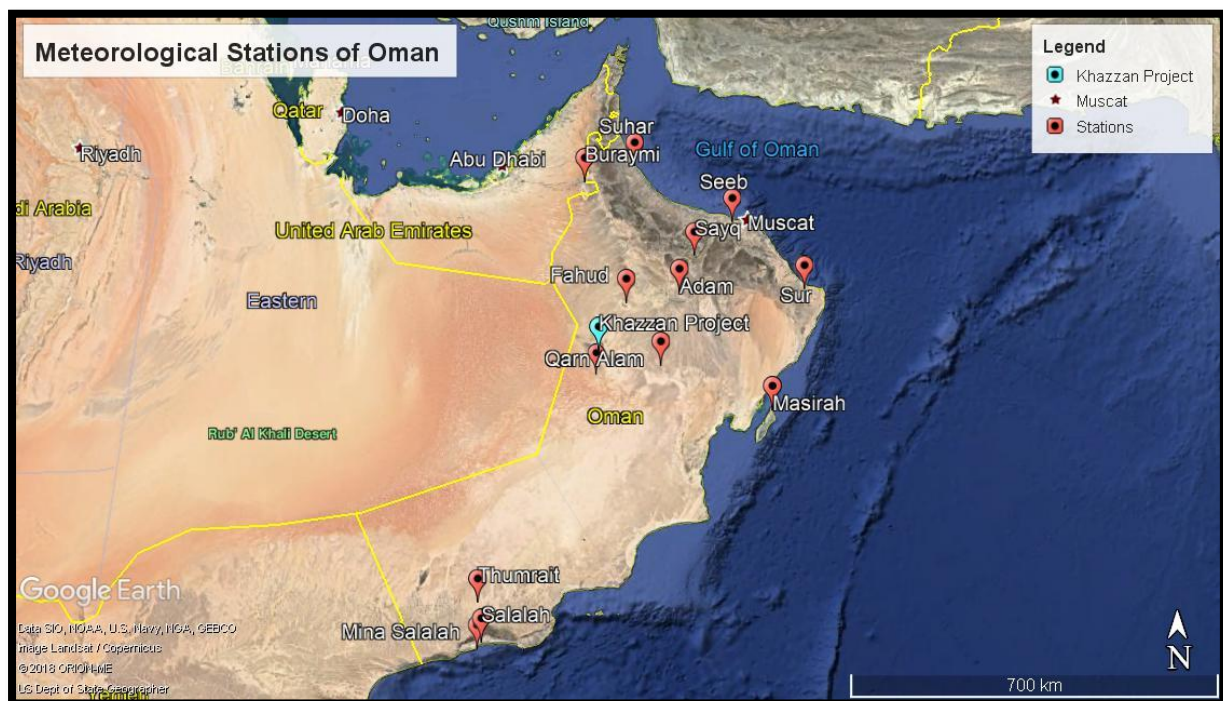
Figure 4: A map representing the 12 weather stations used in this study.

Three stations called Fahud, Adam airport, and Qarn Alam were included as an exception even though they had 28 years (1987-2018), 17 years (2002-2018), and 11 years (2002-2018) of record respectively. They were included as they are in the project area of BP, Ad Dhahirah Governorate, which they are interested in. According to WMO, data completeness is of major importance for analysing extreme meteorological events (Data, 2009). For the sake of high-

quality analysis, they recommend that when examining data that capture extreme events, there should be no more than four missing values per year. In this case, some stations had fewer years of rainfall records with missing values that exceed the limit as per WMO, and Trace values (ex. 0.01) which may affect the results of this study. A possible explanation for the missing data is that perhaps an extreme rainfall event could be a reason why the observation was not made on that day (Data, 2009). There was a challenge dealing with all these data and to deal with this problem, missing values were set to Nan and, Trace values were set to zero.

3.1.2 GPCP data (Gridded data)

Another dataset used is GPCP daily v1.3 precipitation data (Global Precipitation Climatology Project), downloaded from KNMI Climate Explorer. They are gridded data that combine station data with satellite data in a spatial resolution of 1-degree latitude-longitude, and daily timescale from October 1996 to March 2018 (Ncdc.noaa.gov, 2018). Daily gridded data are necessary to examine the spatial variability of precipitation, as well as the extremes (King et al., 2012). As GPCP is interpolated data, it tends to underrate the magnitude of extreme precipitation and the input of such events to the total annual rainfall, as well as it overrates the intensity of low rainfall (King et al., 2012).

3.1.3 Era-Interim Reanalysis Data Set

Another data set used in this study is daily fields of Era-Interim ($0.75° \times 0.75°$), which were downloaded from the European Centre for Medium-Range Weather Forecasts (ECMWF) website. Era-Interim Reanalysis is a product of ECMWF that represents global atmospheric reanalysis with a resolution of 80 km, and a month delay from real-time (Dee et al., 2011). It is built upon a numerical weather prediction model which employs data assimilation of a thorough set of observations, ranging from satellites to radiosondes (Balsamo et al., 2015; Dee et al., 2011). The data assimilation system used to produce it, is a 4-dimensional variational analysis (4D-Var) with a 12-hour assimilation window, covering the period 1979 to April 2018 (Balsamo et al., 2015). It contains analysis and forecasts 4 times per day at 00:00, 06:00, 12:00, 18:00, and 12-hour steps 0, 3, 6, 9, and 12 (Balsamo et al., 2015). A limitation of this dataset is that it also relies on observations, which means a dense network and accuracy of observations will give better results. An advantage of using Era-Interim Reanalysis is that it combines various important climate variables, with only a short time lag (Dee et al., 2011).

3.1.4 CMIP5 Model Simulations and Model Projections

This study uses CMIP5 model simulations and model projections (Coupled Model Inter-Comparison Project, phase 5) from a range of modelling centres, downloaded from the ESGF webpage. They include historical simulations for the period 1850 to 2005, which use realistic past radiative forcings. The historical simulations generate their own random El Niño events as they simulate fully circulating oceans (Liu and Allan, 2013). CMIP5 also includes projections made from 2006 to 2100 for three scenarios, wherein this study only scenario RCP4.5 is used (Representative Concentrations Pathway 4.5). It is a mid-range scenario that maintains radiative forcing at 4.5 Wm^{-2} in 2100 (Thomson et al., 2011). They also include AMIP5 simulations which are atmosphere-only CMIP5 simulations, which have observed SST that represents correctly El Niño timings, and other large-scale variability but not the individual weather events. They cover the period 1979 to 2008 except GISS model that covers the period 1950 to 2010 (Liu and Allan, 2013). A limitation of models is the low resolution, parametrizations which do not allow the presentation of small-scale processes. Another caveat is the possible computational error, that might result in providing wrong projections (Lupo and Kininmonth, 2013).

3.2 Methodology

3.2.1 Comparing station data with gridded data (GPCP)

The first part of the analysis done in this study was to compare the station data with the GPCP data, to configure whether station data and gridded data can capture the extreme rainfall events in Oman. A good quality of extreme weather analysis depends on the method used. In this study two methods were used: the percentile and the Peak Over Threshold (POT) method. The percentile method was used by several studies like the Expert Team on Climate Change Detection and Indices (ETCCDI) to analyse meteorological extremes (Data, 2009). According to ETCCDI, using the percentile method is better when analysing events that hardly occur in a year, rather than analysing events that occur once in a long time. Guhathakurta et al. (2011), analysed extreme events using the POT. According to Data (2009) it is considered a better approach to analyse extreme precipitation.

In the current study, the percentile method was used to show the spatial distribution of extreme events in Oman. The POT method was used to depict a fixed threshold for extreme events recorded by the station data, and the equivalent threshold for the gridded data to make a robust comparison. In addition to that, the POT method is also used to quantify the threshold that is associated with flooding events in Oman.

Percentile Method

The 99.9[th] percentile was calculated for both station data and the equivalent gridded points. There are multiple definitions for percentile, but the one used here is P^{th} percentile where P is a number between 0 and 100 of a list of N precipitation values, that are sorted from the least to the greatest value (Schoonjans et al., 2011). It separates the values into two parts: the lower part contains P percent of the values, and the higher part contains P percent of the remaining values. To obtain the percentile, first, the ordinal rank is calculated and then taking the value from the ordered list that corresponds to that rank (Schoonjans et al., 2011). The equation for the ordinal rank R is:

$$R = \left[\frac{P}{100} \times N \right]$$

Peak Over Threshold Method (POT)

The POT method determines the values that are larger than a fixed threshold chosen by the researcher. The method assumes that every value found above the placed threshold is considered an extreme. It belongs to the Extreme Value Theory which is a statistical method that deals with extreme values and how they deviate from the mean or the probability distribution (Abarbane et al., 1992). The thresholds used for the station data were chosen according to similar research that has been done by Kwarteng et al. (2009). It was also chosen by the results provided by the spatial distribution of the 99.9[th] percentile. After deciding on the fixed threshold to be used, Excel was used to calculate and plot the days exceeding the fixed threshold.

Probability Density Function (PDF)

The probability density function is a function used to show the likelihood of finding a variable like precipitation, in this case, falling within a range of values instead of taking on any one value. Its property is that for any given interval $(m, n]$, the probability of X falling in the interval $(m, n]$, is the area between m and n (Stirzaker, 2007).

$$P\{m < X \leq n\} = \int_{m}^{n} f(x) dx$$

The probability density function was used to display the precipitation values in histograms throughout this research. An inset was also included in the histograms to represent the extreme values that the probability distribution tends to underestimate. Since this study is looking at

extreme precipitation events, it was necessary to represent the tail of the distribution in a different distribution.

Era-Interim Reanalysis

Era-Interim Reanalysis produced by ECMWF was used to plot the synoptic precursors that led to the events that were chosen as case studies in this study (Chapter 4). The data sets available are the analysis that is four times per day: 00:00, 06:00, 12:00 and 18:00, as well as forecasts from 00:00 and 12:00, with 3, 6, 9, and 12-hour steps (see *Figure 5*). For each parameter chosen, the average of 00:00, 06:00, 12:00 and 18:00 was calculated using step 0, which means only analysis was used and not forecasts.
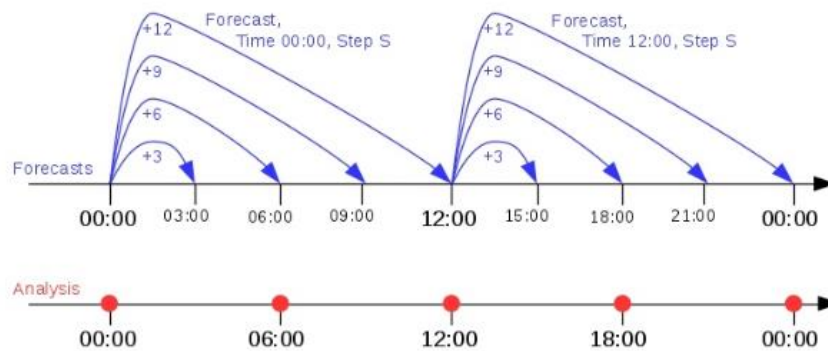
Figure 5: A figure of the Era-Interim data sets that contain analysis and forecasts. Source: (ECMWF Confluence Wiki)

3.2.2 Evaluation of Simulated Extremes and Climate Change Projections

Bias Correction

Three methods of bias correction for the model simulations and model projections were used, to examine which was the best for the data used in this study. Bias correction is an essential method used to correct estimations made by models, especially when it comes to precipitation that has a large spatial variability making it dependent on model resolution (Gutjahr and Heinemann, 2013). A study conducted by Yekambessoun et al. (2016), used three methods for daily precipitation: Linear Scaling, Delta Method, and four types of Quantile Mapping. Their analysis resulted in that the most effective method for daily precipitation was the empirical quantile mapping and the adjusted quantile mapping. Quantile mapping was also applied by Cannon et al. (2015), where they concluded that the method can somehow corrupt the future trends of model projections. After applying the three methods, only one was chosen for giving better results, the empirical quantile mapping method.

In general quantile mapping assumes that the mean and standard deviation of the data are constant with time which is not valid (Piani et al., 2010). However, the method was the most appropriate for the data used. The method is constructed as follows:

$$y = F_{obs}^{-1}(F_{model}(x))$$

Where y is the corrected result, x is the value of the precipitation to be corrected, F_{obs}^{-1} is the inverse of the cumulative distribution function (CDF) of the observations, and F_{model} is the cumulative distribution function of the model (Yekambessoun et al., 2016).

# 4 Observed characteristics of extreme events

This chapter will demonstrate the observed characteristics of extreme events over Oman. A general idea of the rainfall extremes in Oman is provided by calculating the 99.9th percentile of station data and gridded data, and by calculating the days exceeding a fixed threshold that is associated with floods in the area. The next section will be more specific where three stations from two different regions in Oman were chosen to depict the 20 top heaviest rainfall events recorded by station data and gridded data. One region is in Al-Dhahirah Governorate where BP's project is located, so three stations near the area were chosen. The second region is in the northeastern part of Oman where three coastal stations were chosen to make a robust comparison between station data and gridded data. The last section of this chapter presents two case studies where extreme rainfall and flooding took place and affected the two regions mentioned previously. The events will be identified and the synoptic precursors that led to these events will be shown.

4.1 Observed extremes in the region

Figure 6 shows the 99.9th percentile calculation done for the stations shown in *Table 1* and the gridded data. After multiple attempts to find the appropriate percentile that can represent the daily precipitation extremes in Oman, the 99.9th was chosen. Having a look at the map in *Figure 6*, in general, northern Oman receives more rainfall per day than the rest of the country. That can be explained by the fact that the area is surrounded by the highest mountain range of the country which reaches 3139 m as seen in *Figure 1*. On the contrary, the interior desert region and parts of southern Oman receive the lowest daily rainfall. For southeastern Oman, there are also mountain ranges that receive high rainfall as well. As seen in *Figure 6* the three circles representing the cities in southern Oman have low values of daily rainfall, except for one place (Mina Salalah). According to the gridded data map, it receives high rainfall and it can probably be explained by the fact that it is at a higher elevation than the other two surrounding cities (*Table 1*). The results agree with the research done by Al-Hatrushi (2012) and Al Charaabi and Al-Yahyai (2013), where they showed that the spatial distribution of rainfall in Oman is separated into three parts because of its topography.

Table 1: A table showing the 12 weather stations used in this study.

| ID	Name	Latitude	Longitude	Elevation (M)	Period
41254	Saiq	23.07	57.63	1755	1983-2018
41288	Masirah	20.67	58.9	19	1983-2018
41244	Buraimi	24.23	55.78	299	1983-2018
41246	Sohar Majis	24.47	56.63	4	1983-2018
41256	Seeb	23.59	58.28	15	1983-2018
41262	Fahud	22.35	56.48	170	1987-2018
41264	Adam Airport	22.5	57.37	328	2002-2018
41268	Sur	22.53	59.48	14	1983-2018
41275	Qarn Alam	21.38	57.05	133	2002-2018
41312	Mina Salalah	16.93	54.02	25	1983-2018
41314	Thumrait	17.67	54.03	479	1983-2018
41316	Salalah	17.04	54.09	22	1982-2018
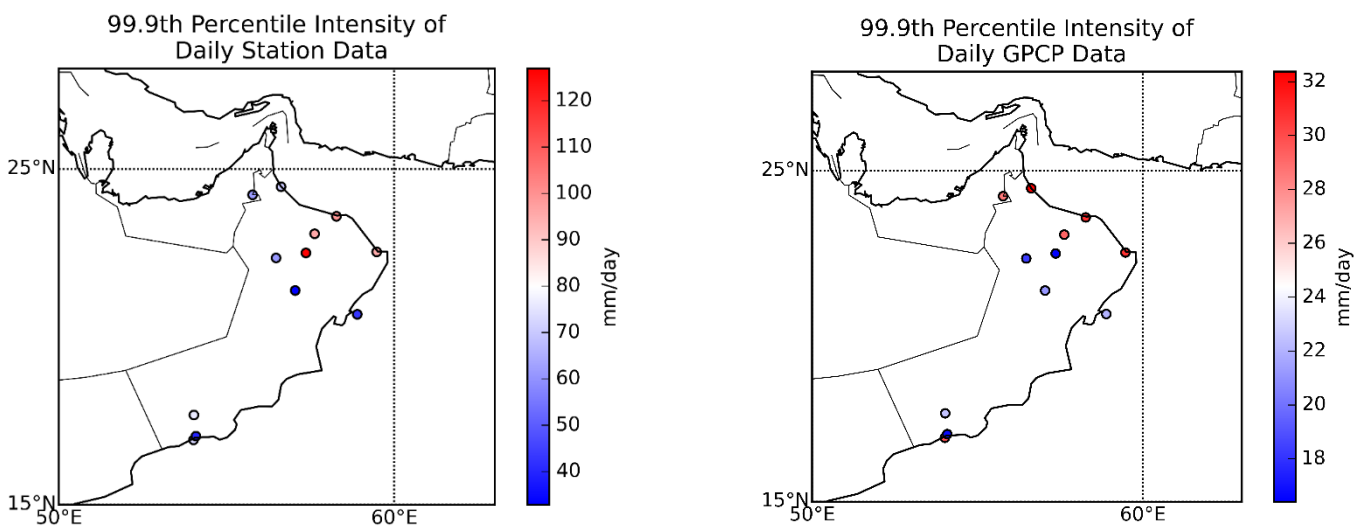
Figure 6: Two maps showing the 99.9th percentile of daily precipitation calculated for the 12 weather stations and the gridded GPCP data used.

According to Kwarteng et al. (2009), rainfall above 50 mm/day for station data is considered extreme rainfall in Oman and it is associated with flood events. This is comparable to the 99.9th percentile of daily rainfall for about half of the stations depicted in *Figure 6* for the daily station data. To pick a fixed threshold for the GPCP data, the results from *Figure 6* were used to estimate the equivalent threshold of extreme events for the gridded data. Taking that into consideration, five fixed thresholds were chosen that represent extreme rainfall events and flooding in Oman.

The graph depicted in *Figure 7*, shows that all 12 stations have had rainy days of 50 mm. The rarest rainfall event that had occurred during this period is 200 mm/day, and it was recorded on one day in only two stations (Masirah island and Seeb) that are coastal areas in northern Oman. A caveat to this result is that not all stations cover the period 1982-2018 as seen in *Table 1*, so there might be more days exceeding those five fixed thresholds. However, in general, the 50 mm/day threshold is common among the stations (at least 5 occurrences in all but one station). In addition to that, stations in northern Oman (Seeb, Sur, and Saiq) are the ones with a higher number of days exceeding the thresholds, followed by stations in southern Oman (Salalah, Mina Salalah, and Thumrait) then the interior region (Buraimi and Qarn Alam).

A comparable variability across station location is followed by the GPCP data but with different magnitudes of thresholds that are lower than the ones used for the station data. That is expected as gridded data are interpolated, so they tend to underestimate the intensity of extreme precipitation and their contribution to the total annual rainfall (King et al., 2012). The maximum fixed threshold of 60 mm was reached by grid points that are located either in northern or southern Oman where the elevation is high. Furthermore, the days exceeding that rate is only one which is apparently events such as thunderstorms and cyclones, where will be shown in sections 4.2 and 4.3.
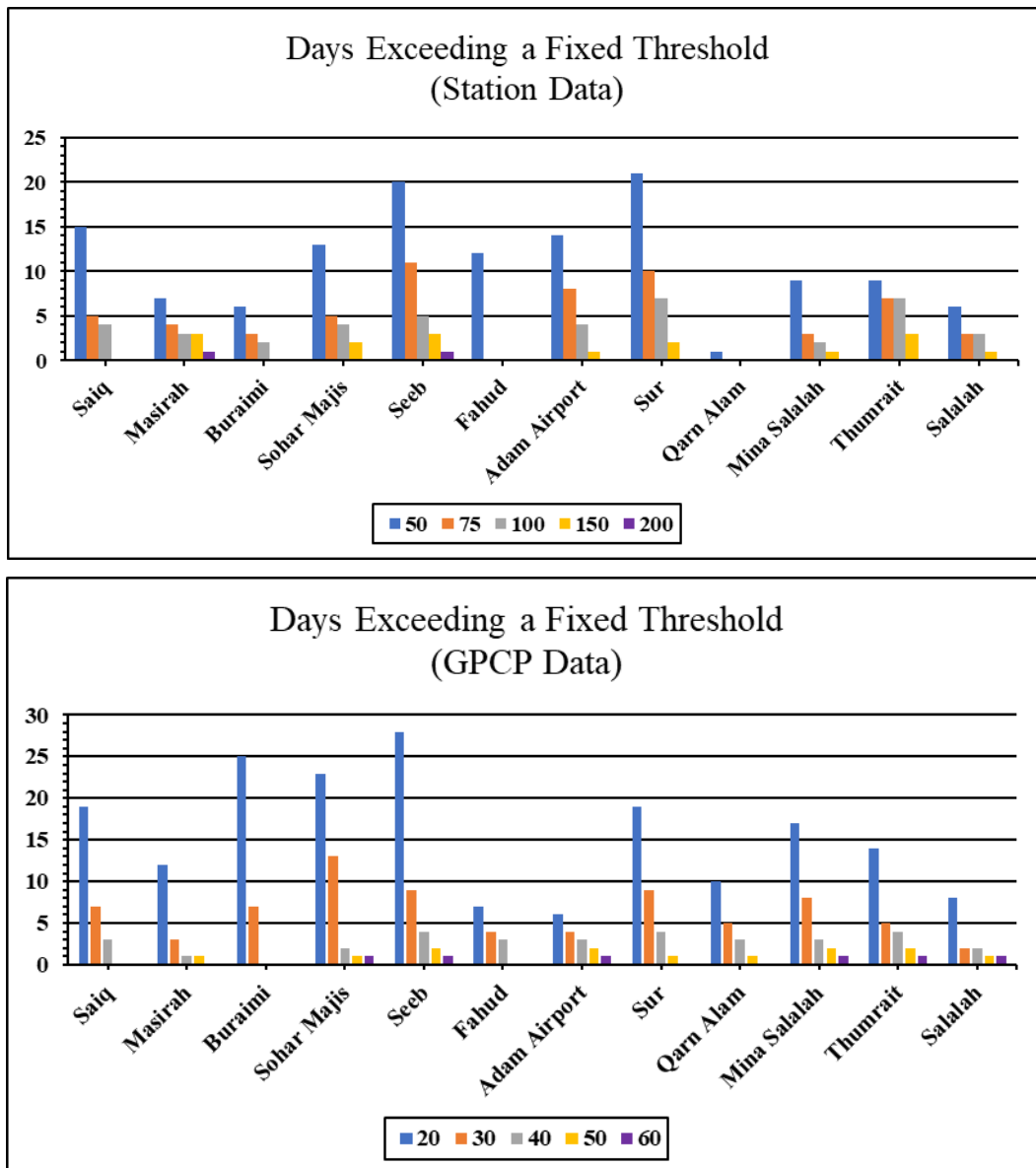
Figure 7: The graphs illustrate the stations and the GPCP daily rainfall data with the days exceeding the five fixed thresholds that are associated with extreme rainfall events in Oman during 1982-2018.

4.2 Case study 1: Ad-Dhahirah March 2016

Ad-Dhahirah is a governorate located in the interior region of Oman, where the Khazzan project is based (*Figure 4*). Three stations near the area were chosen to examine whether the station data and gridded data can capture the extreme event that happened between the 9th and 11th of March 2016, that was mentioned by BP. The stations are Fahud (28 years of data), Adam airport (17 years of data), and Qarn Alam (11 years of data) (see *Table 1*). A common period that is covered by the three stations and gridded data was analysed (2002-2018).

Table 2 and *Table 3* show the top 20 heaviest rainfall events captured by the stations and the gridded data. All stations capture aspects of the 9-11th March 2016 event. For Fahud and Qarn Alam, the station data recorded a higher rainfall rate than the gridded data on the 9th of March 2016. In addition to that, the 10th of March was captured by the station in Qarn Alam, and not by the gridded data. On the contrary, for Adam airport the gridded data recorded a higher rate than the station data on the 9th which is 62.1 mm. This could possibly be explained by the fact that Adam airport, is at a higher altitude than the rest of the two stations (see *Table 1*), and that possibly gridded data can identify heights. Overall for the three areas in *Table 3*, the 2016 event is considered one of the top three events recorded by the gridded data since 2002, which indicates a large-scale event.

Table 2: Top 20 heaviest rainfall events captured by the three weather stations (QAF).

Fahud (Station)	Date	Adam Airport (Station)	Date	Qarn Alam (Station)	Date
69.9	27/12/1999	153.9	12/05/2012	68.3	24/06/2015
62	01/07/1994	128	06/03/2010	31	10/03/2016
62	11/07/1994	121.9	13/04/2010	29.5	09/03/2016
61.7	01/07/1994	110	07/05/2011	24.1	03/02/2017
61	11/07/1994	99.1	03/07/2011	22.6	11/03/2016
61	09/03/2016	99.1	27/07/2011	19.6	17/12/2017
59.9	21/11/1993	95	03/07/2011	15.7	30/01/2016
59.9	22/04/1994	88.9	27/07/2011	13	27/03/2014
59.9	21/11/1993	72.9	02/05/2010	11.9	08/12/2015
59.9	22/04/1994	59.9	06/07/2011	10.7	06/06/2015
59.9	15/10/1993	57.9	05/05/2010	8.4	19/02/2017
55.9	20/11/1993	54.4	04/02/2013	7.1	25/06/2015
50	08/12/1993	53.1	20/04/2010	6.1	05/04/2017
50	20/06/1994	52.1	09/03/2016	5.8	26/03/2014
50	17/08/1994	48	24/03/2010	5.1	28/09/2005
50	15/10/1993	46	19/06/2011	5.1	29/11/2005
31	20/11/1993	45	30/07/2011	5.1	15/06/2014
26.4	08/12/1993	42.9	19/04/2011	5.1	29/12/2014
21.1	20/06/1994	39.9	07/05/2010	4.8	28/09/2005
15.2	17/08/1994	39.9	14/04/2010	4.3	29/11/2005

Table 3: Top 20 heaviest rainfall events captured by the gridded data (QAF).

Fahud (Gridded)	Date	Adam Airport (Gridded)	Date	Qarn Alam (Gridded)	Date
44.3	24/03/1997	62.1	09/03/2016	50.3	12/06/2015
42.1	01/03/2005	50.6	01/03/2005	49.9	24/03/1997
42.1	09/03/2016	45.4	24/03/1997	45.6	09/03/2016
33.1	24/04/2013	32.6	25/06/2007	34.6	04/06/2010
27.5	25/06/2007	24.3	04/06/2010	31	01/11/2011
21.7	08/02/1998	23.3	02/11/2011	28.4	03/06/2010
21.7	23/03/2007	18.3	09/11/1997	23	15/08/2013
18.5	15/04/2003	17.4	19/01/2009	21.4	05/03/2010
18.2	11/03/2002	16.1	15/04/2003	21	20/03/1997
17.9	17/04/2003	15.6	03/02/2013	20.9	29/07/2003
17.5	25/01/1997	15.1	24/04/2013	19.2	09/11/1997
17.2	06/03/2005	15.1	14/04/2003	18.3	23/03/2007
16.2	30/03/2009	14.5	25/01/1997	17	08/02/2010
15.8	20/01/2003	14.3	20/03/1997	16.1	25/06/2007
15.1	22/11/2013	14.2	08/08/2006	15.4	19/01/2009
14.5	02/11/2011	14.1	12/05/2002	14.3	03/02/2013
14.4	25/03/2013	13.8	15/03/1997	14.1	01/08/2012
14.3	12/06/2015	13.6	04/09/2015	13.9	02/11/2011
13.8	29/04/2013	13.3	17/12/2017	13	17/12/2017
13.6	08/04/2016	13.1	07/03/2016	12.1	06/12/2004

Figure 8 illustrates a time series of the station data and gridded data used to examine this event, using the data for the period 2002-2018. The highest event recorded by the gridded data for that period is the 2016 event that is highlighted with a green circle. Furthermore, the gridded data have managed to exceed the average of the station data for the same year. This is considered as an exception where both station data and gridded data agree. As according to Guhathakurta et al. (2011), gridded data are not good at capturing extreme events most of the time, and that station data are better in capturing extreme events. In this case, it did capture the extreme event and even exceeded the station data, it probably means that it was a large-scale event. The same can be seen in *Figure 9,* which shows the precipitation intensity distribution, where the gridded data reach the highest average rainfall rate of 50 mm/day. In general precipitation histograms have a gamma distribution as most of the values are zero, which makes sense as Oman is an arid and semi-arid region. In the histogram a probability of 0.0002 is equivalent to a single occurrence (1 day in the 17-year period).
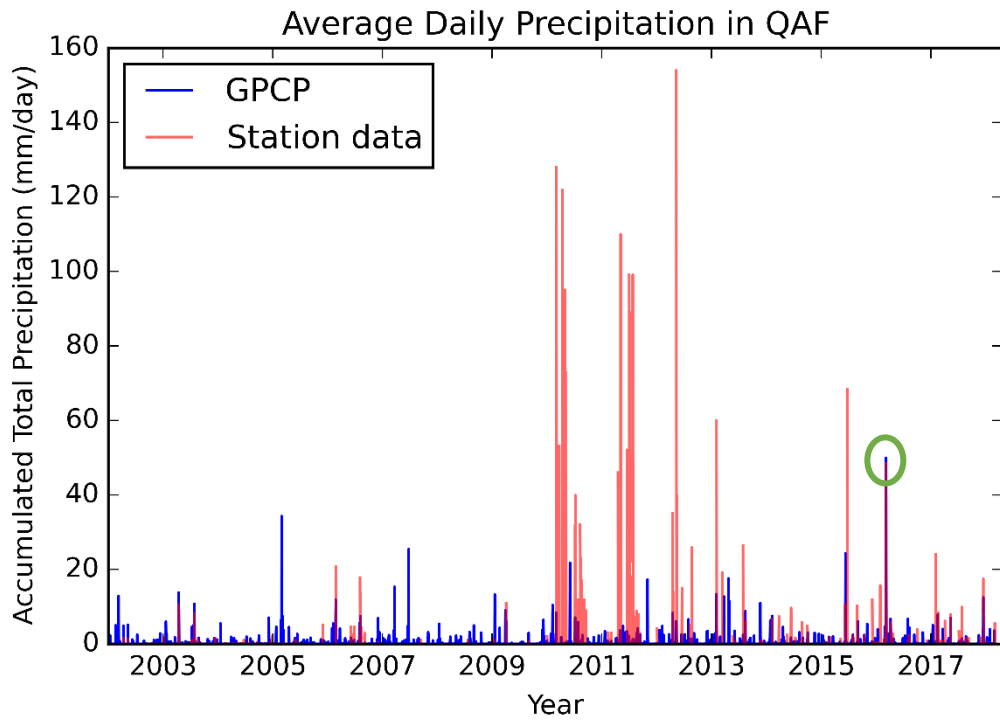
Figure 8: Time series of the daily rainfall (mm/day) averaged for the three stations and average gridded data (GPCP), for the period 2002-2018. QAF stands for Qarn Alam, Adam airport, and Fahud.
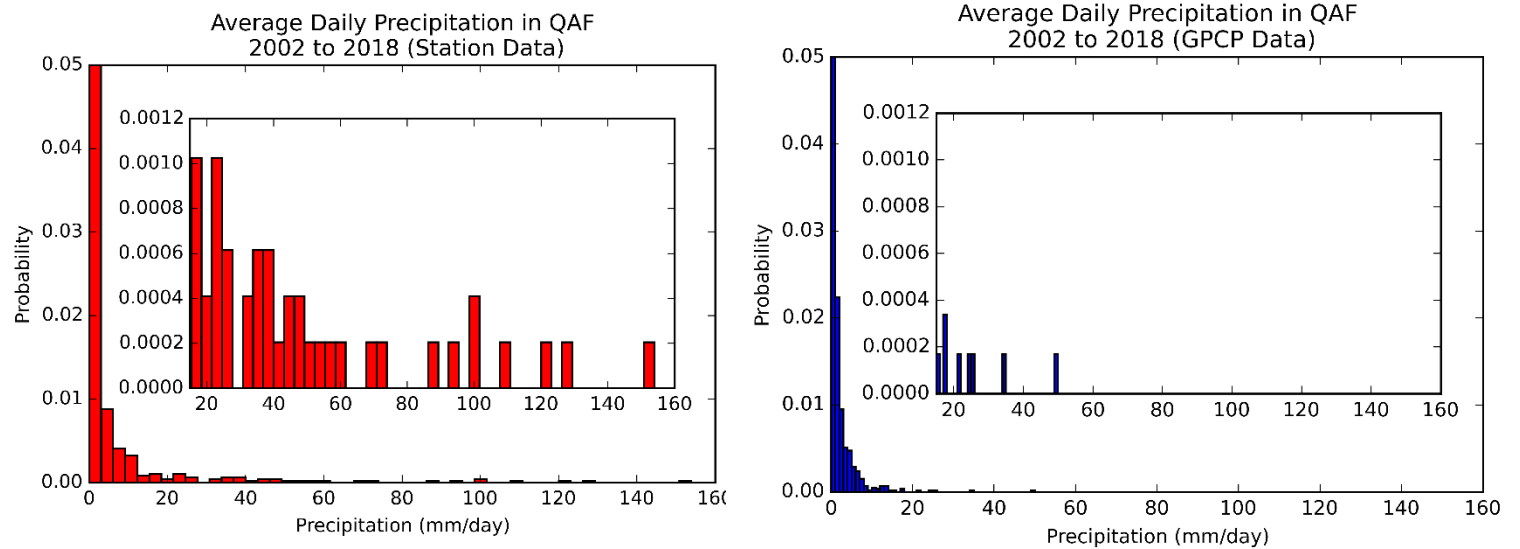
Figure 9: A probability distribution of the daily precipitation intensity for both station data and gridded data for Qarn Alam, Adam Airport, and Fahud over the period 2002-2018. The inset is a zoomed in version of the histogram to show the extreme events that the distribution tends to underestimate. As a result, it is essential to use a separate distribution for this part of data.

To understand what atmospheric conditions were associated with the heavy rainfall and flooding event, some synoptic fields are plotted in the day of the event and in the three days leading up to the event (2-metre temperature anomaly, total column water vapour anomaly, 2-metre dewpoint temperature anomaly, absolute mean sea level pressure, and 10-metre wind speed) using Era-Interim Reanalysis. *Figure 10* starts by plotting the 2-metre temperature anomaly covering the 6th of March up to the 11th.

It seems that there was a gradual drop in the temperature anomaly (5 to -5 Kelvin) in BP's project area (labelled as Khazzan) that becomes obvious on the day of the event (9th) and continues to drop up to the 11th where it starts increasing steadily back again.

Dewpoint temperature can be used as an indicator when the air becomes saturated. So, as the temperature was increasing before and after the day of the event, the dewpoint was expected to decrease as correctly seen in *Figure 11*. The region started showing an increase in the dewpoint temperature that was significant on the 10th and started dropping back gradually by the 11th.

In *Figure 12*, it seems that there is no clear picture of where the water vapour is coming from. However, there is a clear indication that since the 7th, it kept increasing with pick on the 9th. After doing some research on the event, it has been concluded that the first country to be affected by the event was the United Arab Emirates (labelled as UAE in the plots). Low pressure (1003-1008 hPa) passed by UAE first then Oman bringing widespread thunderstorms, hail, strong winds and severe flooding affecting both countries (Times of Oman, 2018). From *Figure 13*, the low pressure can be seen approaching Oman bringing strong winds over the region heading from the Persian Gulf from where possibly the water vapour is coming from (see *Figure 12*). The severe thunderstorm is depicted in the visible satellite image captured by NASA Aqua/Modis (see *Figure 14)*, where the cumulonimbus clouds cover the area on the 9th of March 2016.
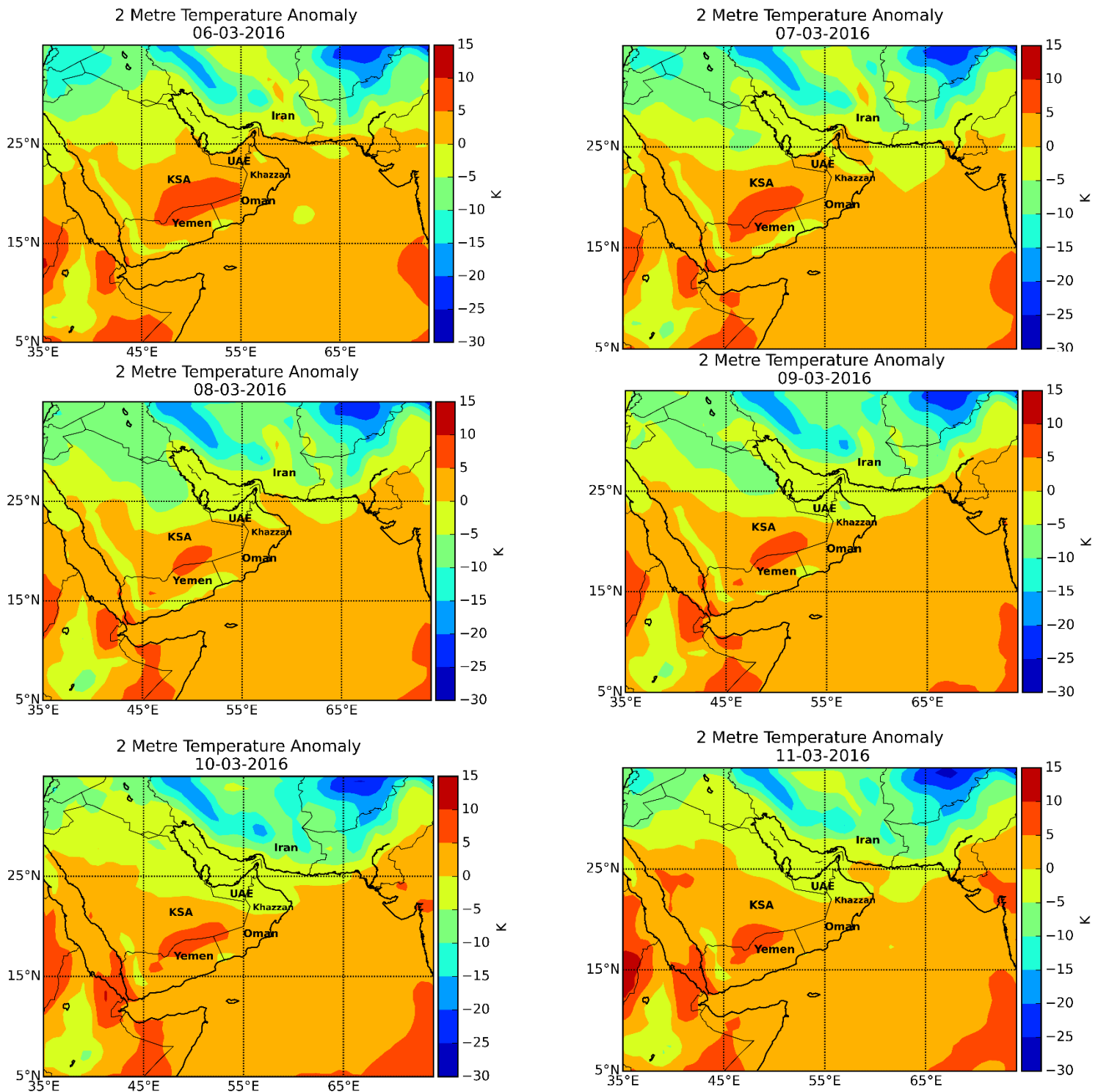
Figure 10: Era-Interim Reanalysis used to explain the synoptic precursors of the March 2016 event. The figure includes the anomalies for 2-metre temperature three days leading to the event and on the day of the event itself. The plots indicate a drop in the temperature gradually in BP's project region (labelled as Khazzan) from the 6th of March up to the 11th where it starts increasing back again.

24
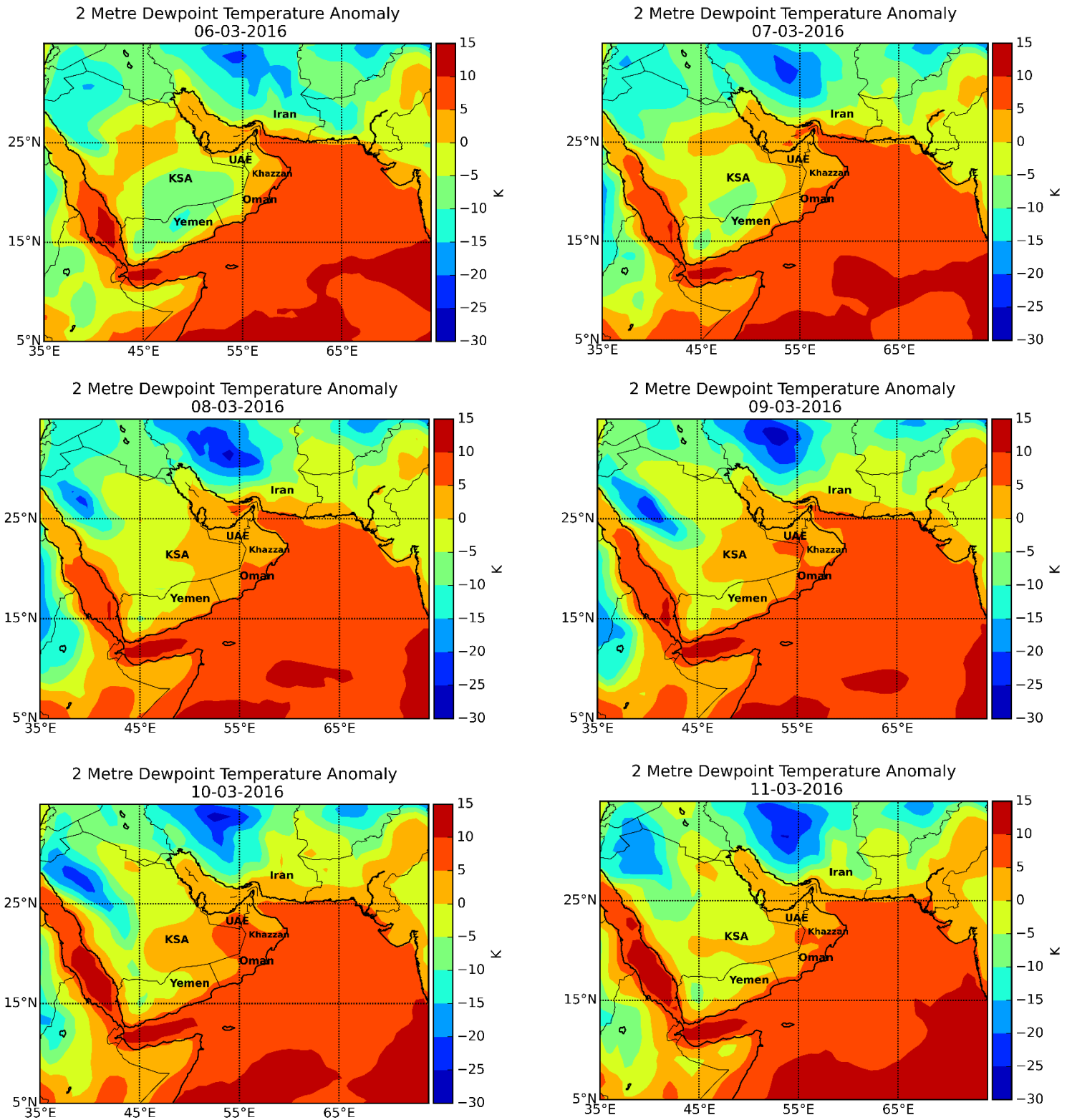
Figure 11: Era-Interim Reanalysis used to explain the synoptic precursors of the March 2016 event. The figure includes the anomalies for 2-metre dewpoint temperature three days leading to the event and on the day of the event itself. The plots indicate an increase in the dewpoint temperature gradually in BP's project region (labelled as Khazzan) from the 6th of March up to the 11th where it starts decreasing back again.
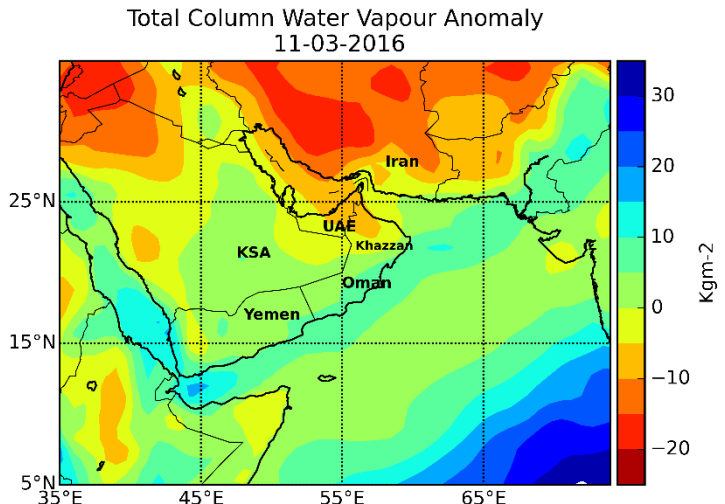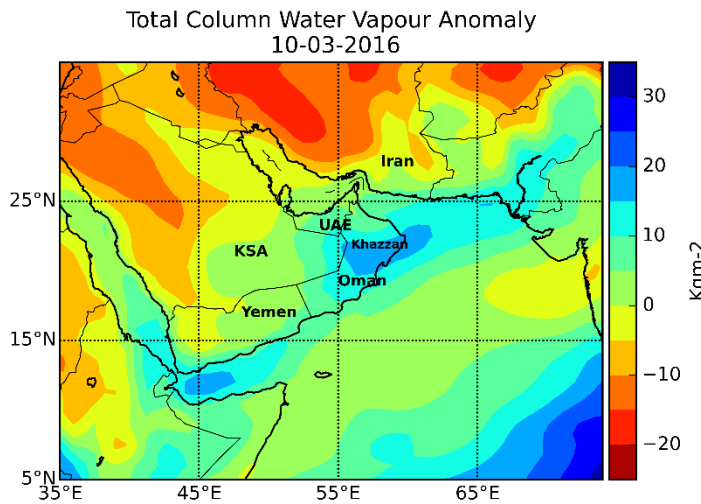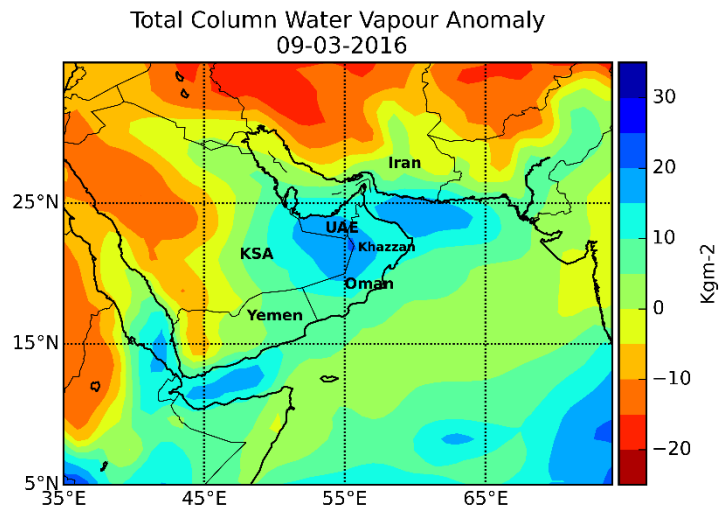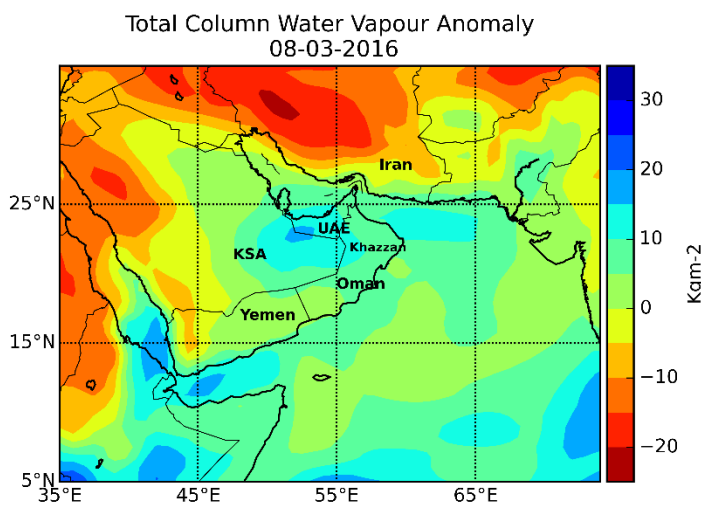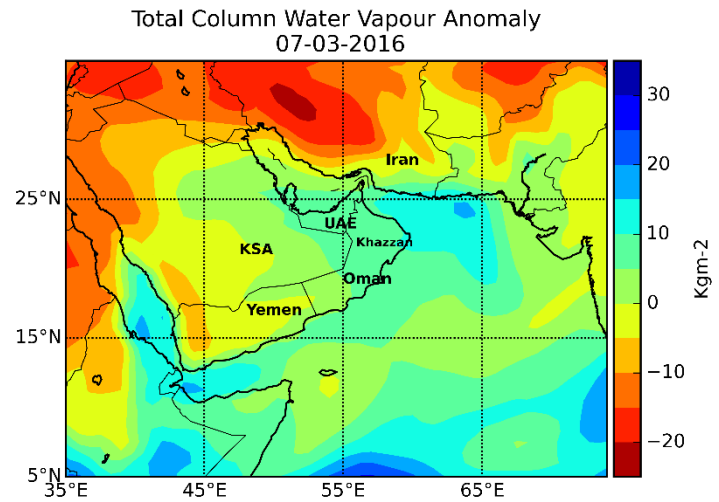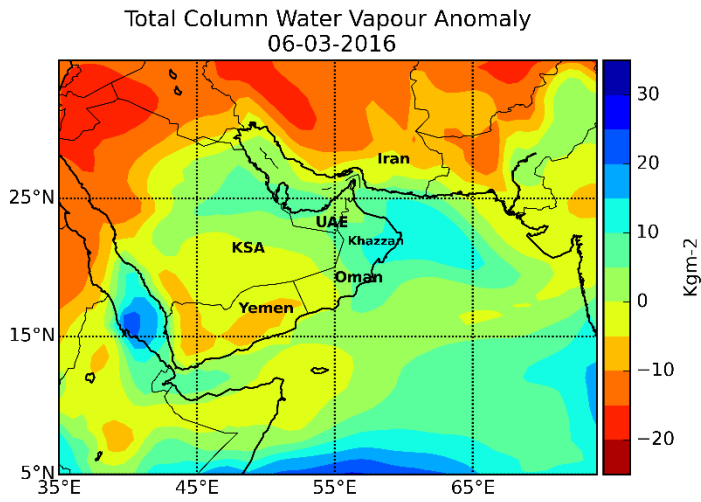
Figure 12: Era-Interim Reanalysis used to explain the synoptic precursors of the March 2016 event. The figure includes the anomalies for the total column water vapour three days leading to the event and on the day of the event itself. The plots indicate an increase in the water vapour gradually in BP's project region (labelled as Khazzan) from the 7th of March up to the 11th where it starts decreasing back again.
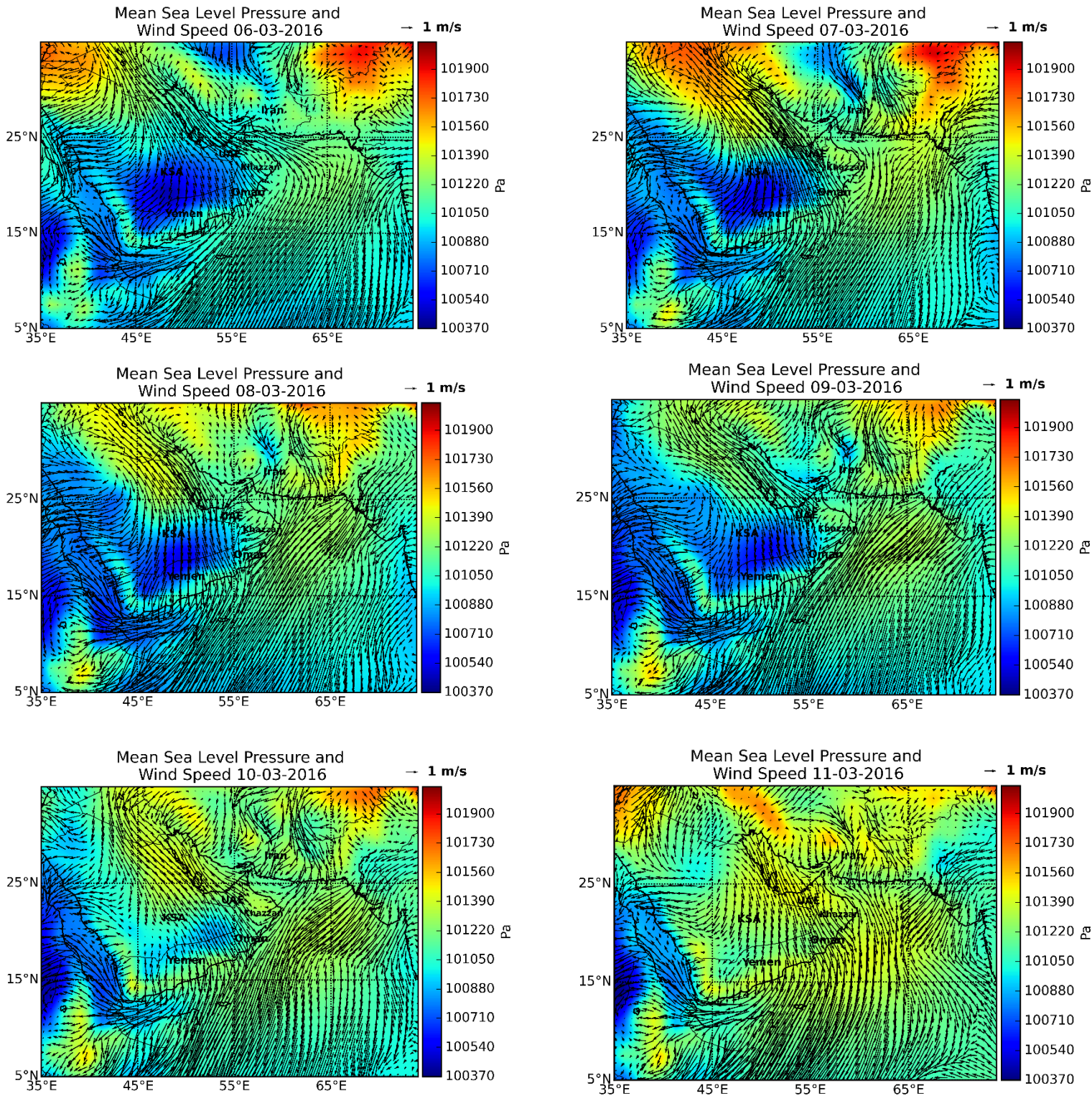
*Figure 13: Era-Interim Reanalysis used to explain the synoptic precursors of the March 2016 event. The figure includes the anomalies for the total column water vapour three days leading to the event and on the day of the event itself. The plots show the low pressure (in blue) that approaches steadily Oman and the strong winds accompanied from the Persian Gulf (narrow area between KSA and Iran).*
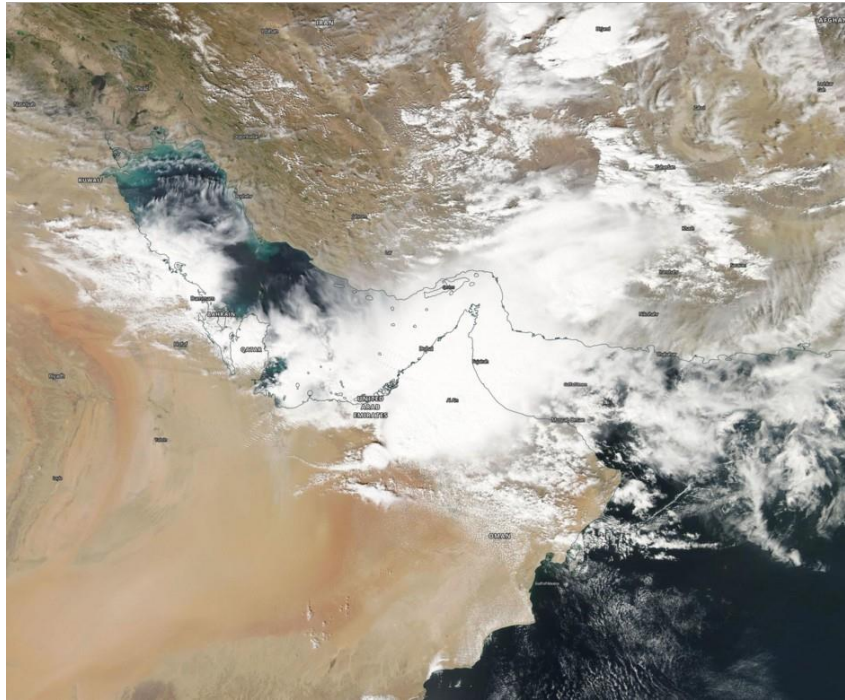
Figure 14: Weather conditions over the Arabian Peninsula on March 9, 2016 shown using a visible image. Source: NASA Aqua/MODIS.

4.3 Case study 2: Cyclone Phet June 2010

Another case study that was examined is cyclone Phet that affected northeast of Oman on the 3rd and 4th of June 2010. By the time the cyclone had dissipated from Oman, it caused enormous flash floods and heavy rain that reached 603 mm, which is five times the annual rainfall of Oman. Furthermore, it caused 50 deaths and damage worth about 4.2 billion US dollars in Oman (Haggag and Badry, 2012). Three stations near the area were chosen to examine whether the station data and gridded data captured the event. The stations are Masirah Island (36 years of data), Sur (36 years of data), and Seeb (32 years of data) (see *Table 1*). A common period that is covered by the three stations and gridded data was analysed (1996-2018).

Table 4 and *Table 5* show the top 20 heaviest rainfall events captured by the stations and the gridded data. For Sur and Seeb, the station data recorded a higher rainfall rate than the gridded data on the 3rd and 4th of June 2010. On the contrary, for Masirah Island, the gridded data recorded a higher rate than the station data on the 3rd which reached 51.4 mm. In addition to that, the 4th of June was not captured by the station data for Masirah. This could possibly be explained by the fact that Masirah Island is in a higher altitude than the rest of the two stations (see *Table 1*), and that again as in case study 1 could possibly mean that gridded data can identify heights. As well as Masirah was the first place in Oman to be affected by the cyclone. Surprisingly, overall for the three areas in *Table 5*, the 2010 event is considered one of the

highest events recorded by the gridded data since 1996 in comparison to the station data that had even higher events.

Table 4: Top 20 heaviest rainfall events captured by the three weather stations (MSS).

Masirah (Station)	Date	Sur (Station)	Date	Seeb (Station)	Date
209.3	12/06/2015	178.1	09/02/1994	249.9	03/04/1992
170.9	09/08/1997	163.1	05/11/1990	199.9	18/03/2008
162.1	18/01/1992	144	12/12/1986	150.1	02/02/1995
84.8	30/07/2003	135.9	24/01/1990	135.9	16/09/1993
70.1	21/11/1997	134.1	05/01/1994	127	05/08/1998
59.9	20/11/1997	120.9	20/03/1994	99.8	21/01/2011
54.1	22/07/1995	117.1	04/06/2010	99.1	24/12/2004
42.9	11/06/1996	96	10/01/1994	99.1	04/06/2010
41.9	15/03/1987	82	28/03/1992	98	24/12/2004
41.1	11/11/2011	80	12/09/1992	85.1	04/06/2010
40.9	14/03/1995	66	26/12/1995	78	07/12/1986
39.4	01/11/2011	63.5	03/06/2010	70.1	25/12/1995
35.1	28/01/1992	62	12/07/1994	67.1	15/12/1995
33	11/08/1983	59.9	21/04/1991	66	05/04/1992
33	04/10/1992	53.1	12/06/2015	63	09/06/1998
29.7	11/08/1983	52.1	27/06/1993	61	22/07/1995
27.9	04/10/1992	52.1	20/06/1994	58.9	13/02/2014
25.1	11/06/2015	51.1	27/06/1993	56.9	23/06/1983
24.6	18/12/1996	51.1	20/06/1994	55.9	26/03/1997
22.1	03/06/2010	51.1	15/06/1991	51.3	21/06/1994

Masirah (Gridded)	Date	Sur (Gridded)	Date	Seeb (Gridded)	Date
51.4	03/06/2010	52.9	06/06/2007	60.4	31/05/1997
34.1	09/11/2011	49.8	05/06/2007	59.6	01/03/2005
31.5	01/11/2011	43.9	04/06/2010	44.7	06/06/2007
26.5	04/06/2010	43.6	31/05/1997	40.4	09/03/2016
26.2	05/06/2007	39.4	06/12/2004	34.9	04/06/2010
24.9	18/06/2007	35.6	01/03/2005	33.6	17/04/2003
23.6	31/10/2011	34.2	03/06/2010	33.4	24/04/2013
22.4	08/07/2011	32.6	01/04/2009	31.4	23/02/2006
21.8	11/06/2015	30.5	09/11/2011	30.7	15/03/1997
21.3	01/03/2005	28.6	07/02/2010	28.6	07/02/2010
21.3	25/03/1997	27.7	25/06/2007	26.2	14/04/2003
20.8	10/10/1999	27.4	09/03/2016	26.2	18/03/2007
18.2	09/11/1997	27.2	25/03/1997	25.9	25/03/1997
17.7	12/06/2015	26.1	21/03/2017	24.8	22/11/2013
16.9	29/07/2003	25	08/07/2010	24.5	16/03/1997
16.4	25/03/2013	24.4	15/04/2003	24.1	08/04/2016
15.9	09/03/2016	24	15/04/2012	23.9	12/02/1999
15.9	24/03/1997	23.5	17/01/1997	23.3	07/03/2016
15.8	18/04/2012	22	07/03/2016	23	31/03/1998
15.8	27/05/2013	19.8	01/03/2016	22.5	02/11/2011

Figure 14 illustrates a time series of the station data and gridded data used to examine this event, using the data for the period 1996-2018. One of the highest events recorded by the gridded data for that period is the 2010 event that is highlighted with a green circle. However, in comparison to case study 1 section 4.2, the gridded data did not manage to exceed the average of the station data for the same year, though it is a cyclone. It is expected that gridded will usually not capture extreme events, and in this case, the amount of average rainfall recorded by station data was almost double the gridded. The same can be seen in *Figure 15* where the gridded data reach one of the highest average rainfall rates approximately 40 mm/day for the 2010 event. In addition to that, 1 day in 22 years corresponds to a probability of 1 day per 8400 days, approximately 0.0001. Apart from that, the histograms also show what King at al. (2012) concluded in their research, that gridded data underestimate the extreme events and overestimate the intensity of low events.
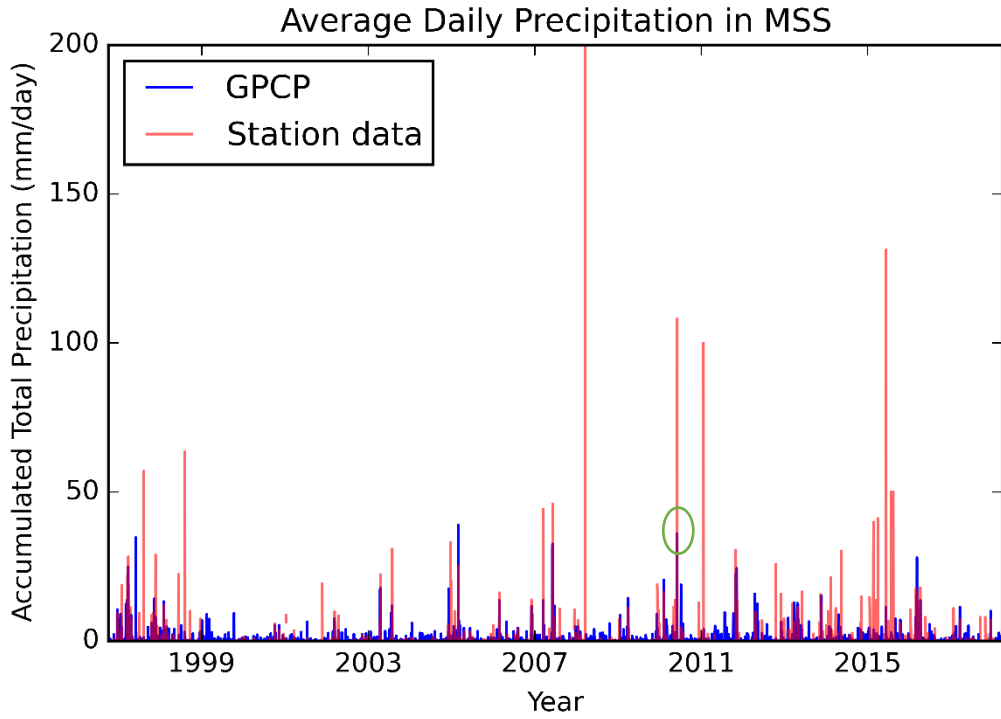
Figure 15: Time series daily rainfall for the average three station data and average gridded data (GPCP), for the period 1996-2018. MSS stands for Masirah, Sur, and Seeb.
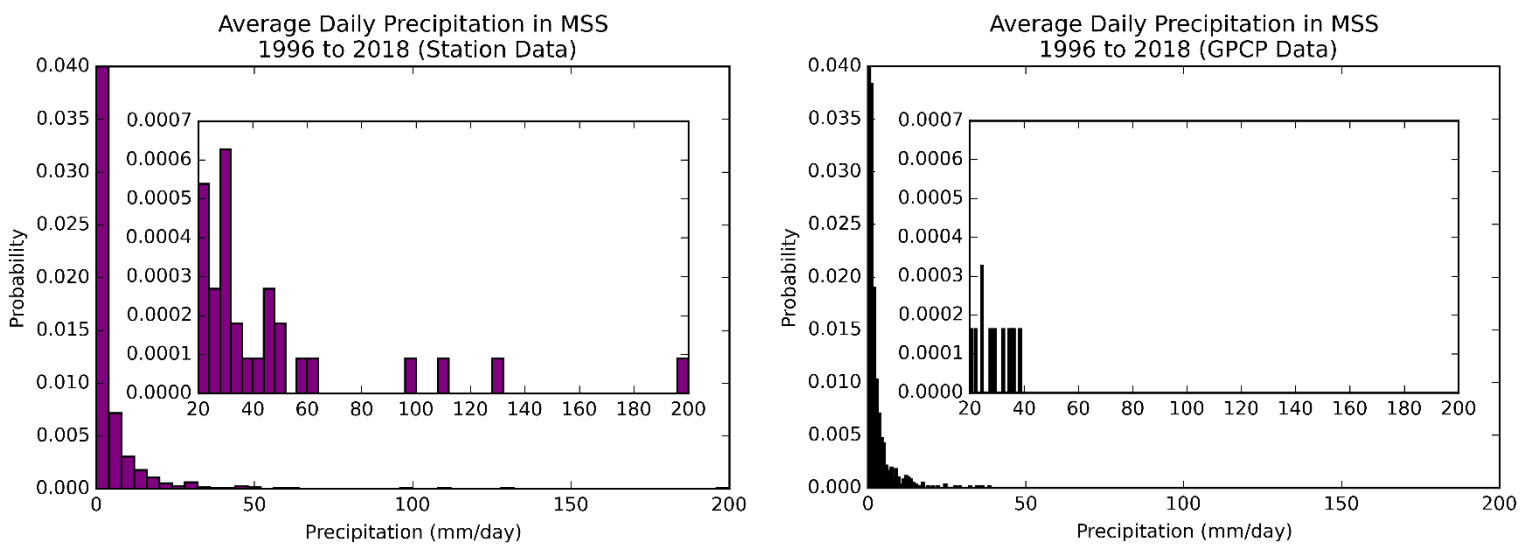
Figure 16: A probability distribution of the daily precipitation for both station data and gridded data for Masirah, Sur, and Seeb cities. The inset is a zoomed in version of the histogram to show the extreme events. As a result, it is essential to use a separate distribution for this part of data.

To understand what atmospheric conditions were associated with the 2010 cyclone event, some synoptic fields are plotted in the day of the event and in the three days leading up to the event

as already done for case study 1 in section 4.2, using Era-Interim Reanalysis. *Figure 17* starts by plotting the 2-metre temperature anomaly from the 31st of May up to the 4th of June. Three days before the event there was a gradual drop in the temperature anomaly throughout the days and decreases dramatically on the 4th of June.

Looking at the dewpoint temperature anomaly in *Figure 18*, there is a steady increase of the dewpoint temperature anomaly on the east coast of Oman. The dewpoint temperature anomaly ranges from 0 to 5 Kelvin mostly starting from the 31st of May to the 3rd of June, and peaks on the 4th where the anomalies range from 5 to 10 Kelvin from the monthly climatology.

Figure 19 depicts elevated water vapour amount associated with a cyclone heading from the Arabian Sea to the east coast of Oman. The cyclone lands in Oman on the 3rd of June accompanying a large amount of water vapour that deviates from the monthly climatology by approximately 20 to 50 kgm^{-2}.

A low pressure (996-1003 hPa) develops in the Arabian Sea on the 31st of May with strong winds forming a large-scale air mass that spins inwards. It landed on the east coast of Oman with strong winds on the 3rd of June, and by the 4th of June it occupied northern Oman and started heading towards Iran and Pakistan. As depicted in the visible satellite image (see *Figure 21*), on the 4th of June various vigorous thunderstorms were embedded in the centre of the cyclone in northeastern Oman. Cyclone Phet's constant winds for that day were 150 knots, and a total of heavy rainfall that reached 50 mm/hour (Haggag and Badry, 2012).
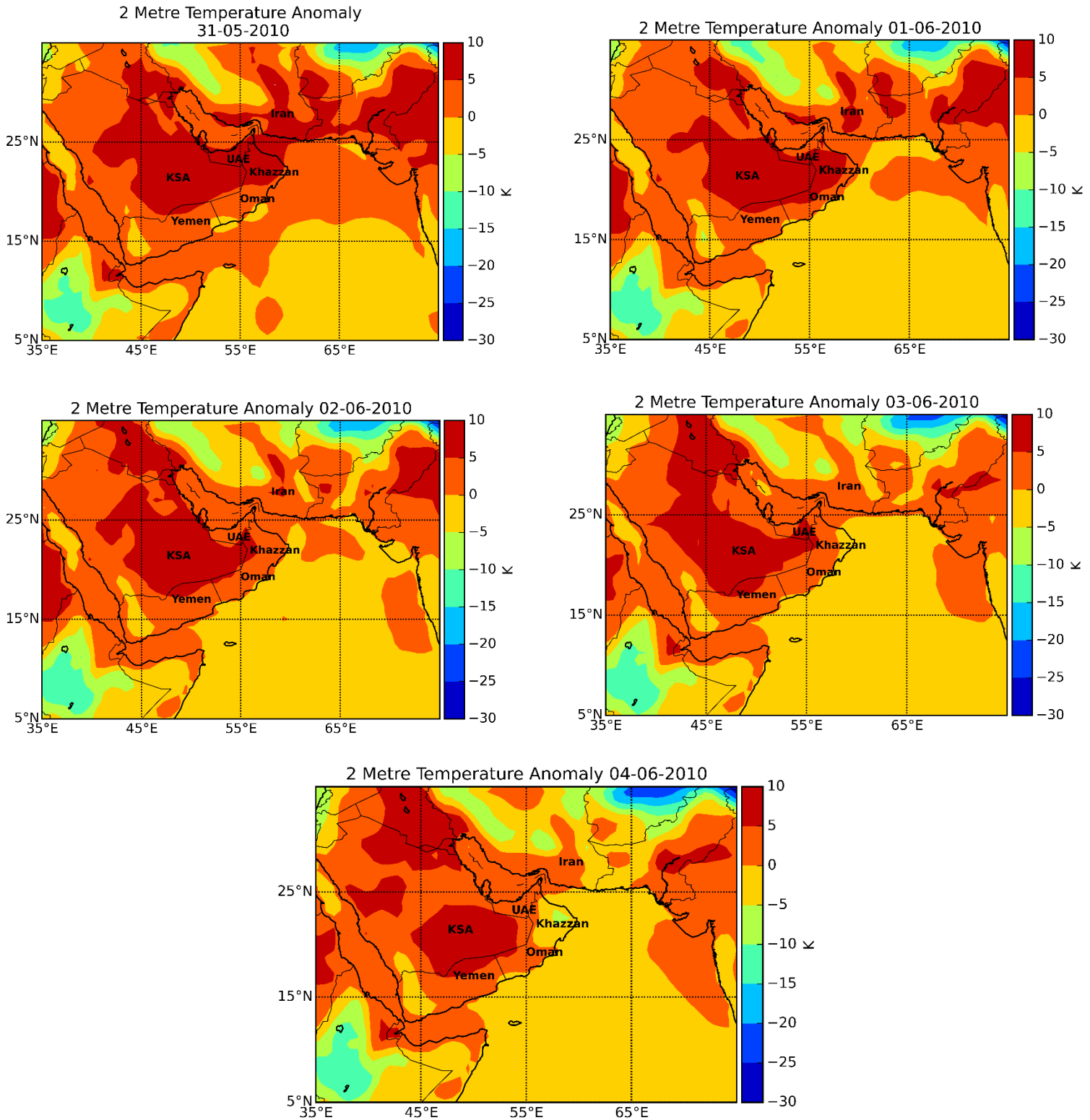
Figure 17: Era-Interim Reanalysis used to explain the synoptic precursors of the cyclone event on June 2010. The figure includes the anomalies for 2-metre temperature three days leading to the event and on the day of the event itself. The plots indicate a drop in the temperature gradually in northeastern Oman from the 1st of June up to the 4th where it drops dramatically.
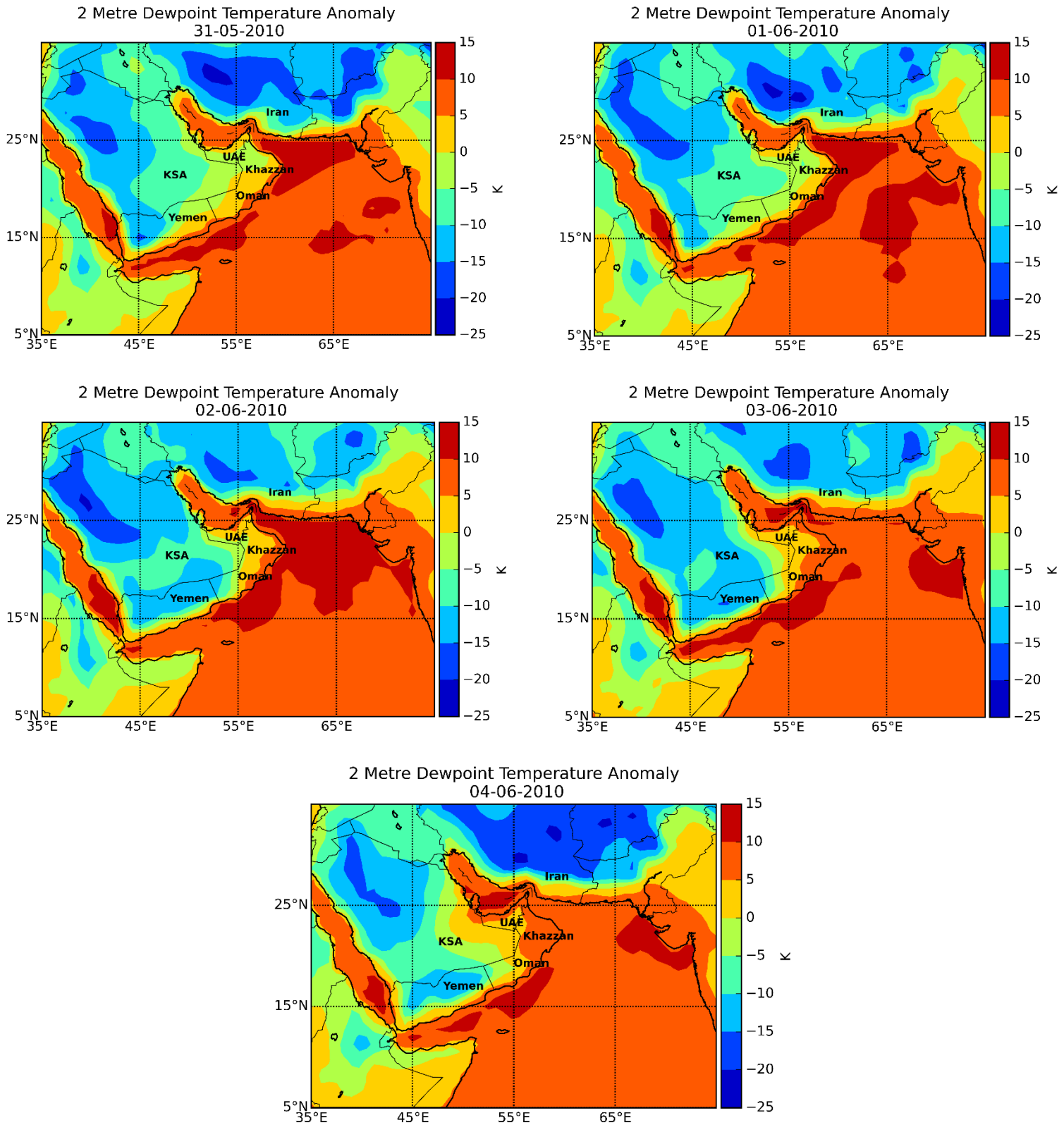
Figure 18: Era-Interim Reanalysis used to explain the synoptic precursors of the June 2010 event. The figure includes the anomalies for 2-metre dewpoint temperature three days leading to the event and on the day of the event itself. The plots indicate an increase in the dewpoint temperature gradually in northeastern Oman from the 1st of June up to the day of the event.
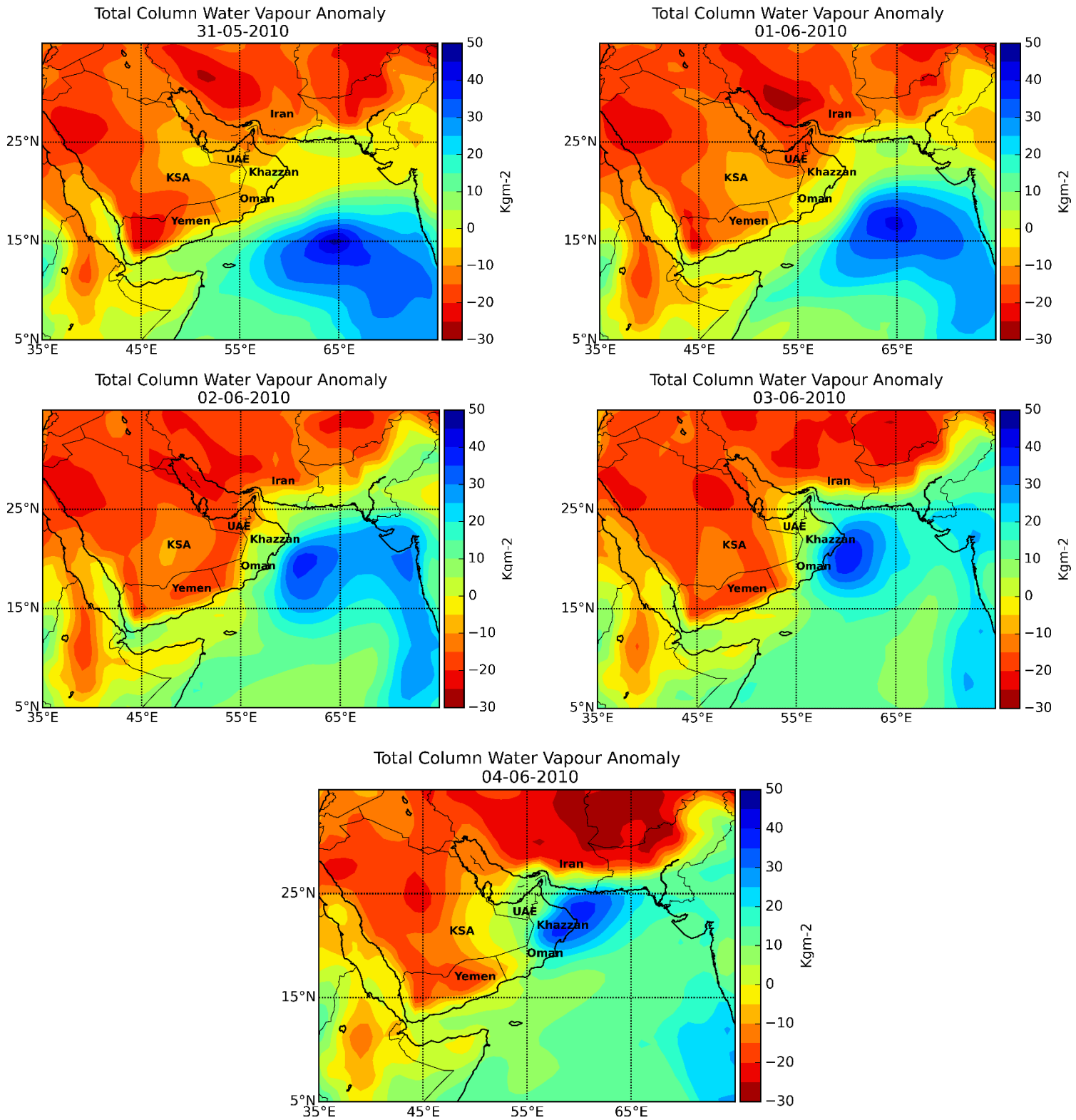
Figure 19: Era-Interim Reanalysis used to explain the synoptic precursors of the June 2010 event. The figure includes the anomalies for the total column water vapour three days leading to the event and on the day of the event itself. The plots indicate an increase in the water vapour gradually in northeastern Oman approaching from the Arabian Sea from the 31st of May up to the day of the event.
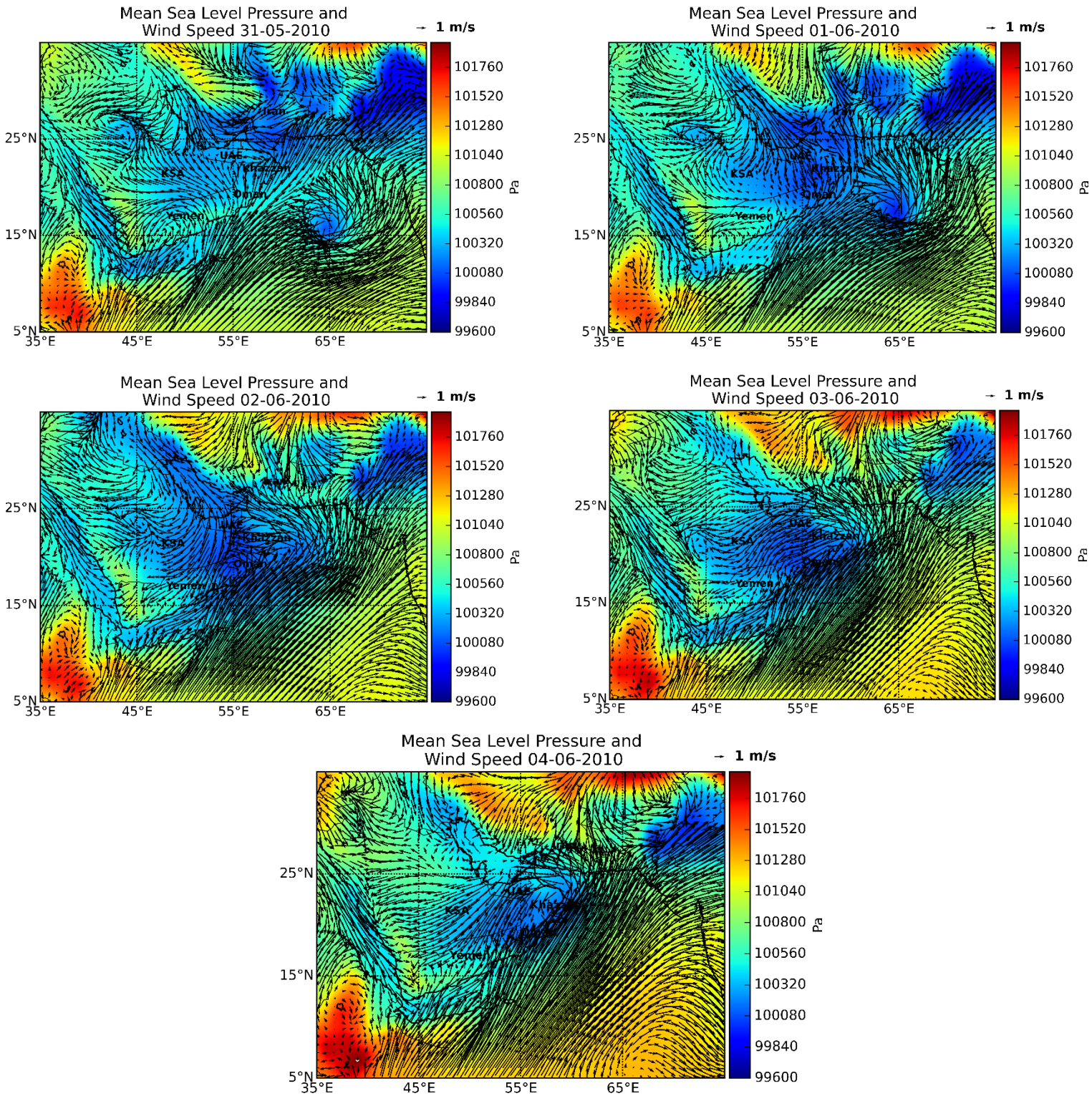
Figure 20: Era-Interim Reanalysis used to explain the synoptic precursors of the June 2010 event. The figure includes the absolute mean sea level pressure and 10 – metre wind speed three days leading to the event and on the day of the event itself. The plots indicate a very low pressure approaching from the Arabian Sea, accompanied with strong winds gradually increasing in northeastern Oman from the 1st of June up to the day of the event.
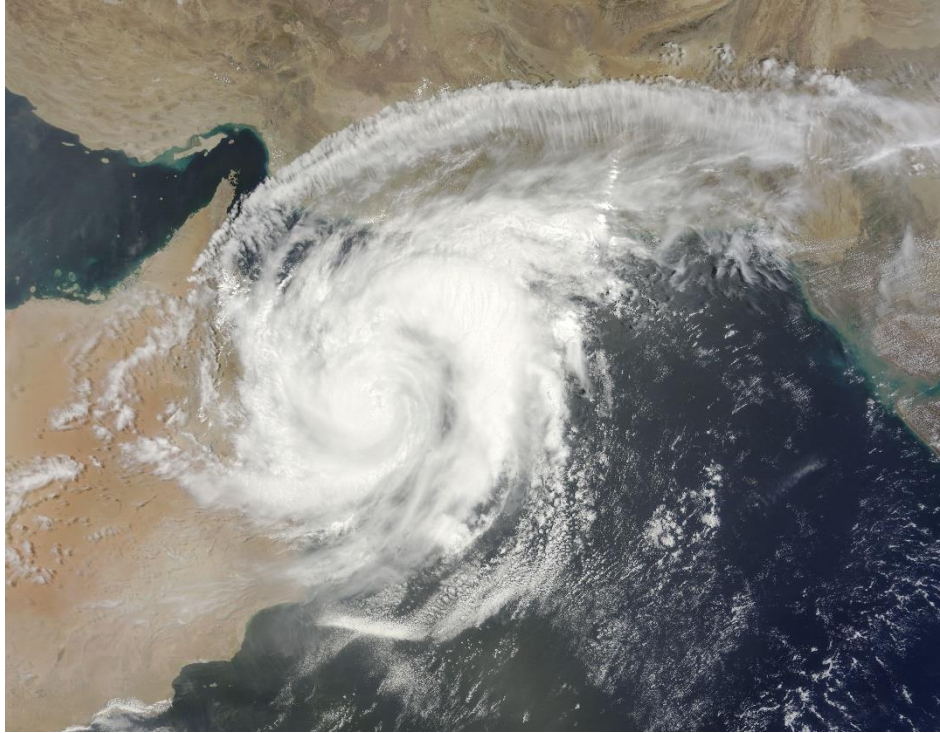
Figure 21: Weather conditions over the Arabian Peninsula on June 4, 2010. Source: NASA Aqua/MODIS.

Summary

The concluding remarks from this chapter are that in general according to literature, gridded data captures some extreme rainfall events, but the magnitude is not always larger enough. They also tend to underestimate the intensity of heavy rainfall and overestimate the intensity and frequency of low rainfall (Guhathakurta et al., 2011; King et al., 2012). By examining the 12 weather station data that cover most parts of Oman and the closest gridded points, the 99.9[th] percentile was calculated. The result from *Figure 6*, was that there is an agreement between the station data and gridded data regarding the spatial distribution of extreme rainfall in Oman. The days exceeding a fixed threshold for both station data and the equivalent for gridded data was then calculated, to check which amount of daily rainfall is associated with extreme rainfall events and possible flooding. The lowest threshold considered for station data is 50 mm/day and 20 mm/day for gridded, and the highest threshold is 200 mm/day and 60 mm/day for the station data and gridded data respectively.

Two events were chosen in this study to investigate, using a case study approach, how well station data and gridded data represent the intensity of extreme events. The March 2016 event is considered an exception where both GPCP and station data agree, and capture the large-scale event, with gridded data even exceeding on average the amount of rainfall captured by the

station data. The cyclone event represents a classic behaviour expected from the gridded data not to capture the extreme events, even though it is a large-scale event. In addition to that, the station data exceeding on average the amount of rainfall captured by the gridded data. However, in both case studies, regarding the gridded data, the two events were considered among the highest rainfall events captured by GPCP from 1996 to the present.

5 Evaluation of Simulated Extremes

This chapter evaluates the simulated extremes of the AMIP and Historical simulations for six CMIP5 models. In the first section, a comparison is done by looking at the variability and histograms of both simulations and GPCP. In the second section of this chapter, a "correction" method is proposed for simulations to make them represent observed extremes.

5.1 AMIP and Historical Simulations

The first thing to be done before evaluating the model simulations is to see whether gridded data can represent station data. In *Figure 22*, a comparison is being done for both station data and gridded data for the period 1999-2005. A probability of 0.0005 is equivalent to a single occurrence (1 day in the 6-year period). As already shown in chapter 3, the gridded data tend to smooth out the extreme precipitation events, and they underestimate the intensity. During the period 1999-2005, the average extreme precipitation according to the station data had reached above 20 mm/day. However, for the gridded data the highest average precipitation reached below 20 mm/day.

For the same period, six CMIP5 models were examined to see whether they captured the same magnitude of precipitation events with the observations. Four out of the six model simulations (HadGEM2, CanAM4, BCC-CSM1, and CNRM-CM5) showed that AMIP provides higher precipitation values in comparison to the historical simulations (see *Figure 23*). This result is expected as AMIP simulations have observed sea surface temperature (SST) so represent correct El Niño timings, and other large-scale variability but not the individual weather events In contrast to that, historical simulations generate their own random El Niño events as they simulate fully circulating oceans (Liu and Allan, 2013). The other two models (GISS and MRI-CGCM3) however, show higher precipitation values in the historical simulations in comparison to the AMIP.

All models, however, represent biases as they show higher values than the observations. The closest model to the observations, both station data and gridded, is the Canadian model (CanAM4 and CanESM2) in *Figure 23*, which is also close to the variability depicted by the GPCP in *Figure 22*. The two models that failed to represent the observations are BCC-CSM1 and GISS, as both AMIP and historical showed very high values. The HadGEM2 and MRI-CGCM3 models failed to represent the probability and variability of daily precipitation for that period, when at the same time the GISS model overestimates the probability and variability.
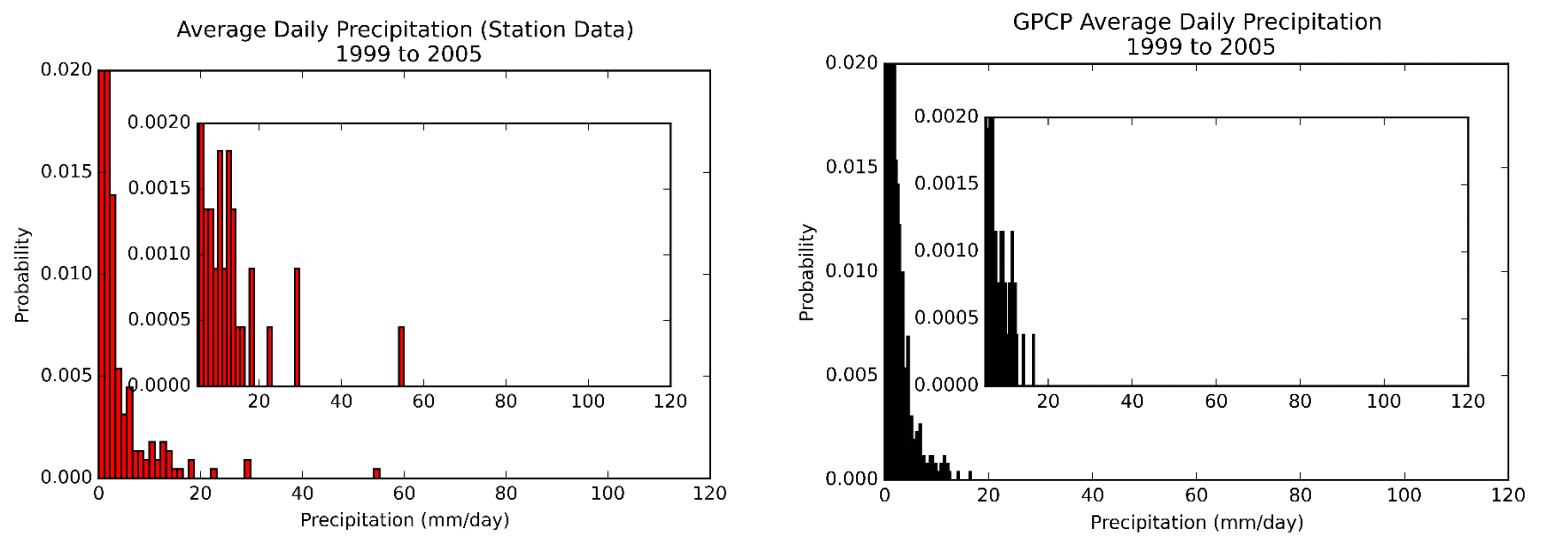

Figure 22: A comparison between the average station data and the average gridded data for the period 1999-2005.
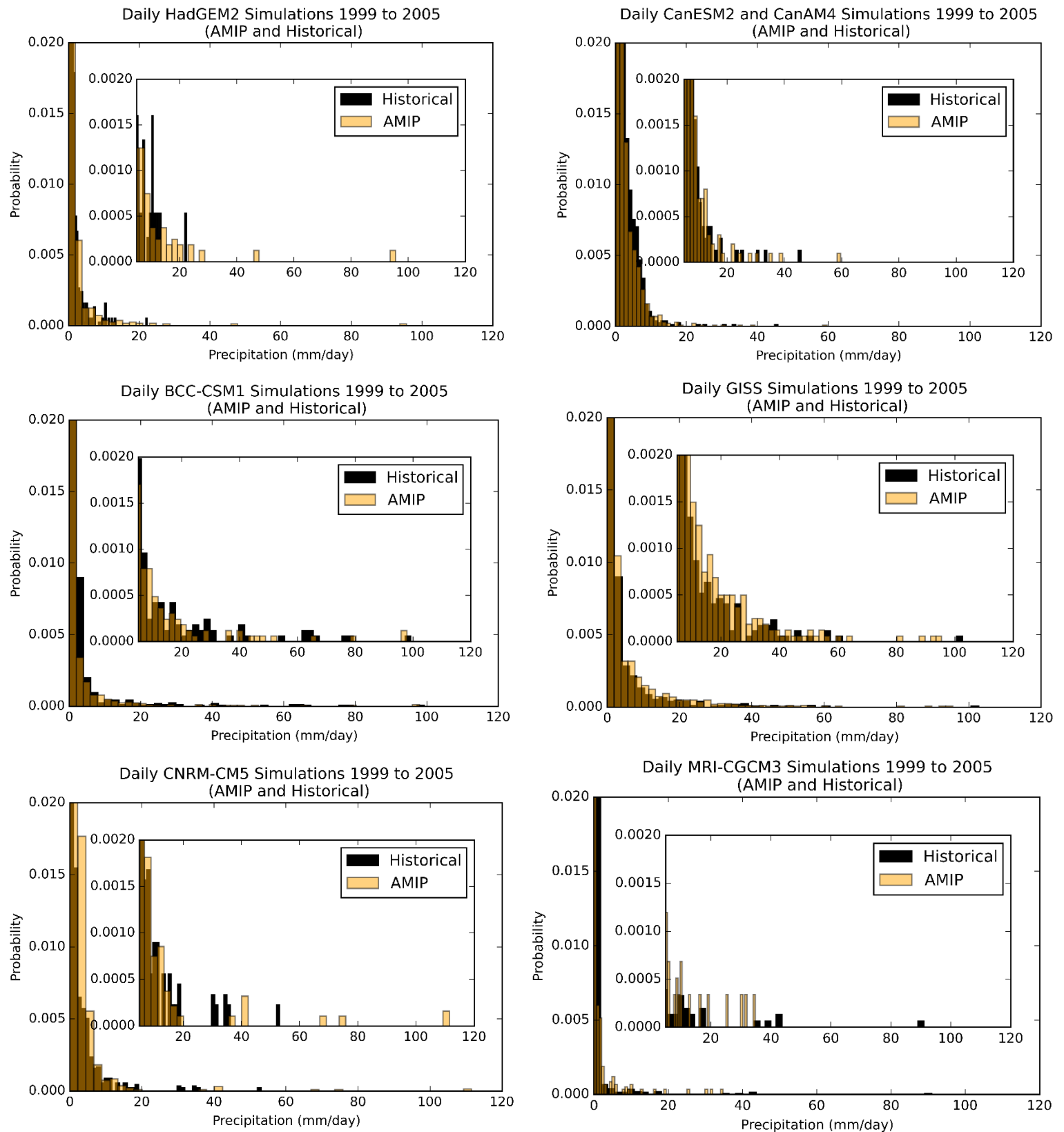
Figure 23: The evaluation of six CMIP5 model simulations (AMIP5 and Historical), and how they represent the extremes in the period 1999-2005. The inset is a zoomed in representation of the extreme events that cannot be seen in the distribution.

5.2 Bias Correction of Model Simulations

To correct the model biases, three methods were applied but one was finally chosen as it gave better results that agree with similar research that has been done. The models were also corrected by considering first the station data and then GPCP, to see which result matched better with reality and the bias correction methods. The three methods used were the linear scaling method, the delta method, and the quantile method, but only the empirical quantile method was finally chosen. The same methods were followed by Yekambessoun et al. (2016), where they proved that the empirical quantile method was the most suitable method for daily precipitation data. After using both station data and GPCP as a reference to correct the model simulations, only the GPCP were finally used to correct the models. The decision to choose the gridded data instead of the station data was difficult as multiple factors needed to be tested to make the right decision.

As previously shown in chapter 2, gridded data captured the extreme events in the case study of cyclone Phet, but it did not capture the magnitude as the station data did. However, in the case of March 2016 event, the gridded data performed much better than the station data which was not expected. In addition to that, as was previously shown in *Figure 6*, the gridded data managed to represent the spatial distribution of the extreme events like the station data. Another factor that helped in considering the GPCP data, is the fact that the station data used in this study had lots of missing days and years. That was evident when the station data were used as a reference to correct the models, where some models showed that the corrected result was even higher than the observations, which does not satisfy the purpose of bias correction. That raised the suspicion that in this case station data cannot be used as a reference to correct the model simulations. On the contrary, the GPCP data were well represented and the correction seemed reasonable as shown in *Figure 24*. The empirical quantile method was finally considered as it gave much better results for the data used, and according to literature, it is suitable for stochastic variables like precipitation (Piani et al., 2010).

Although the quantile mapping method is the best method for the data used, it has the disadvantage that it considers that the mean and standard deviation do not change with time, which is not valid (Cannon et al., 2015). Furthermore, it depends on many degrees of freedom and may not be fixed due to possible overfitting (Gutjahr and Heinemann, 2013). In *Figure 24* the bias correction method done for the six model simulations gave satisfactory results in removing the biases. However, after the bias correction, the probability and variability are smoothed out. Similar results have been shown by Gutjahr and Heinemann (2013), where they

concluded that the risk of bias correction sometimes can be the reduction and modification of the climate change signal (CCS).
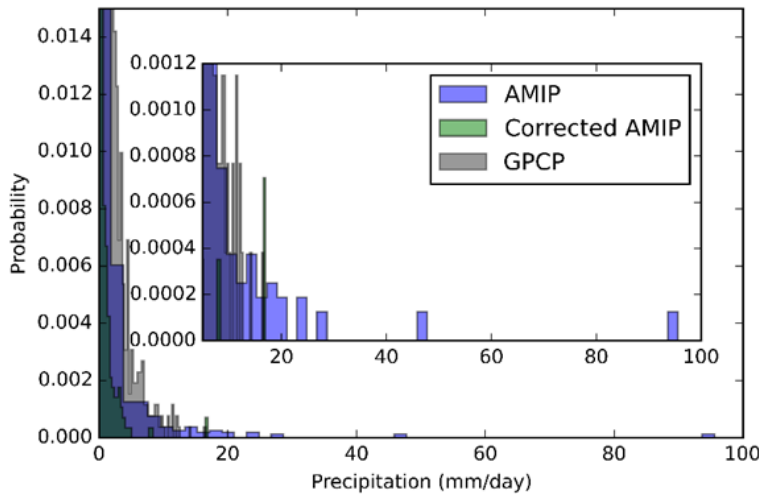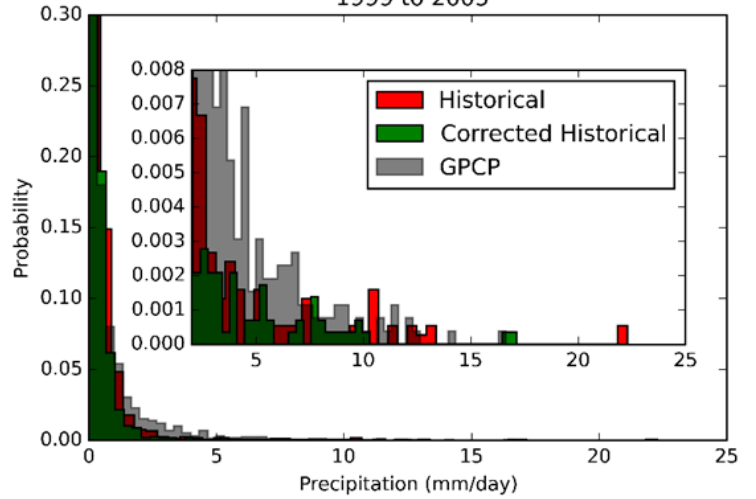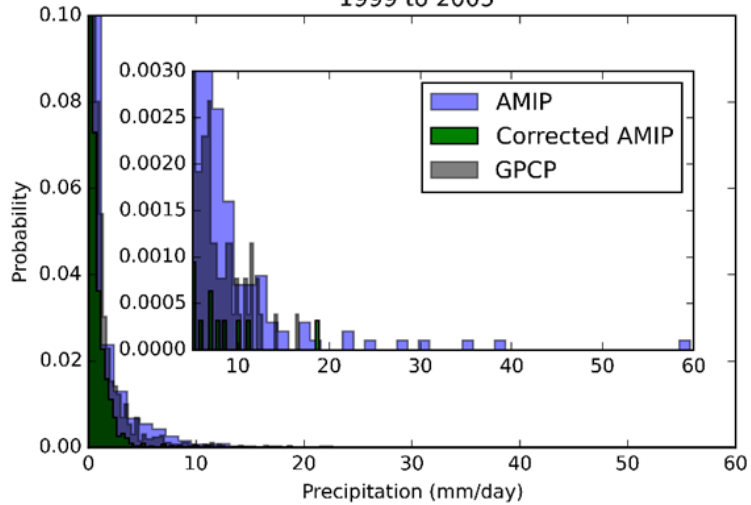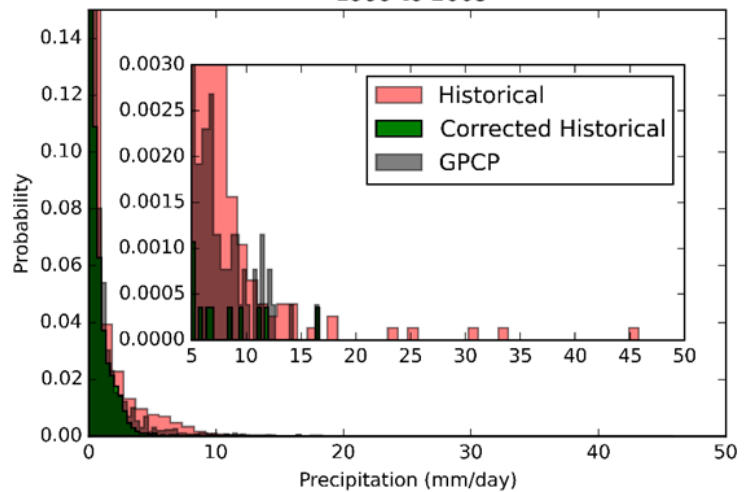
Bias Correction of BCC-CSM1 AMIP Simulation 1999 to 2005
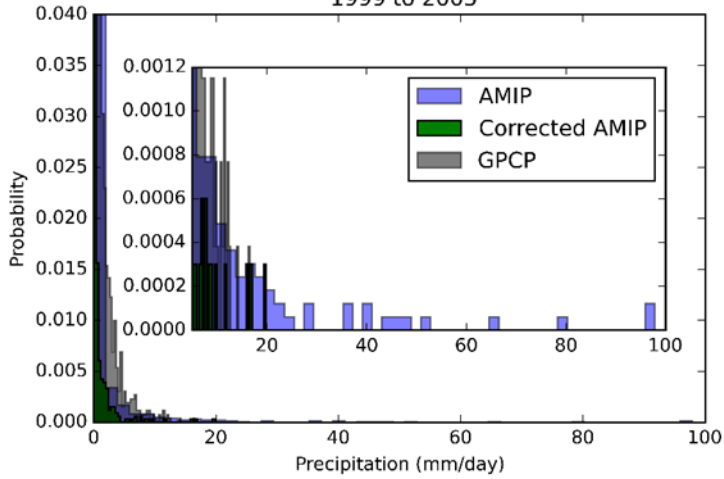
Bias Correction of BCC-CSM1 Historical Simulation 1999 to 2005
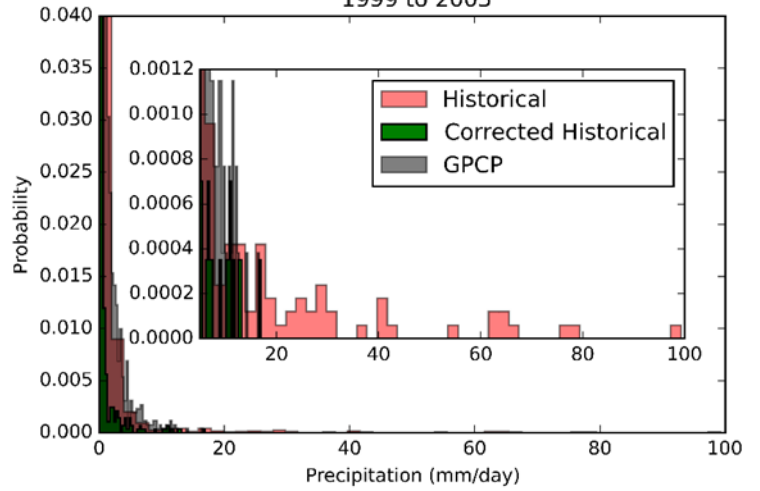
Bias Correction of CNRM-CM5 AMIP Simulation 1999 to 2005
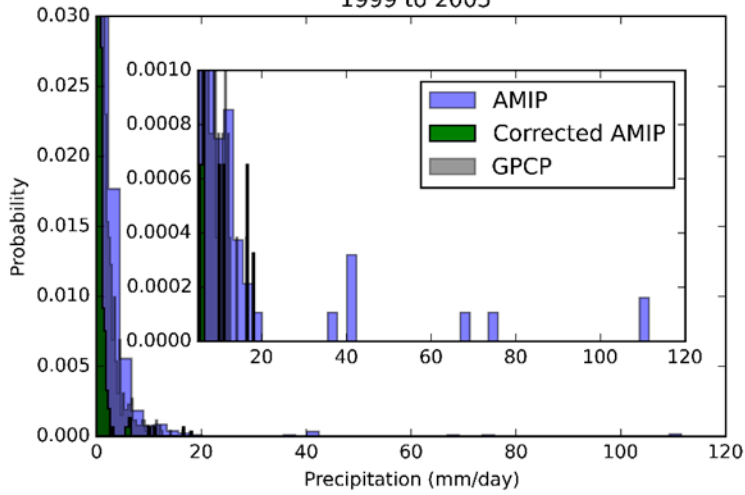
Bias Correction of CNRM-CM5 Historical Simulation 1999 to 2005
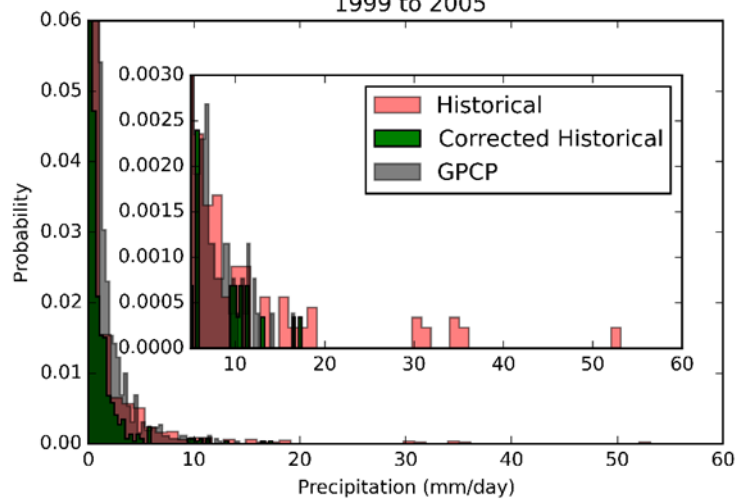
Bias Correction of GISS AMIP Simulation 1999 to 2005
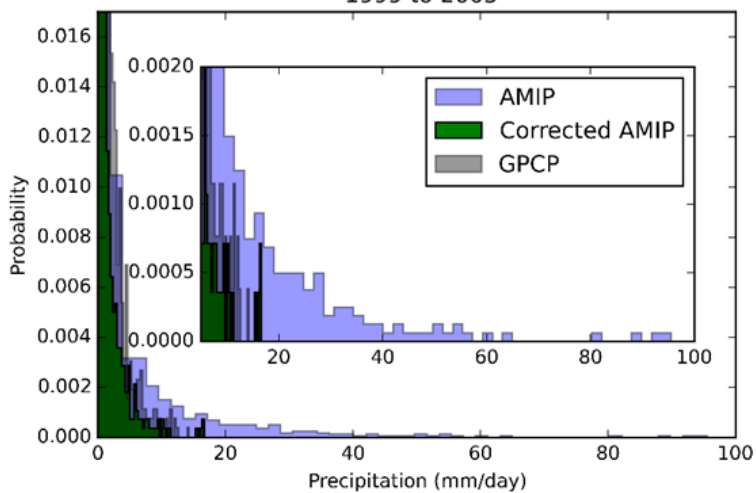
Bias Correction of GISS Historical Simulation 1999 to 2005
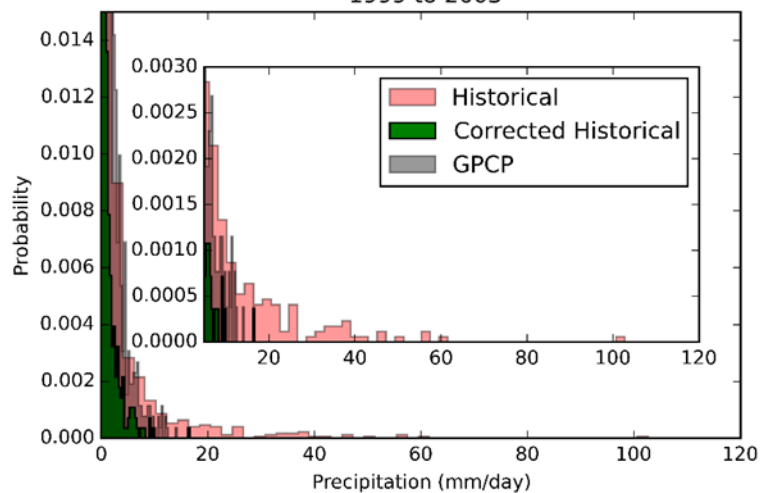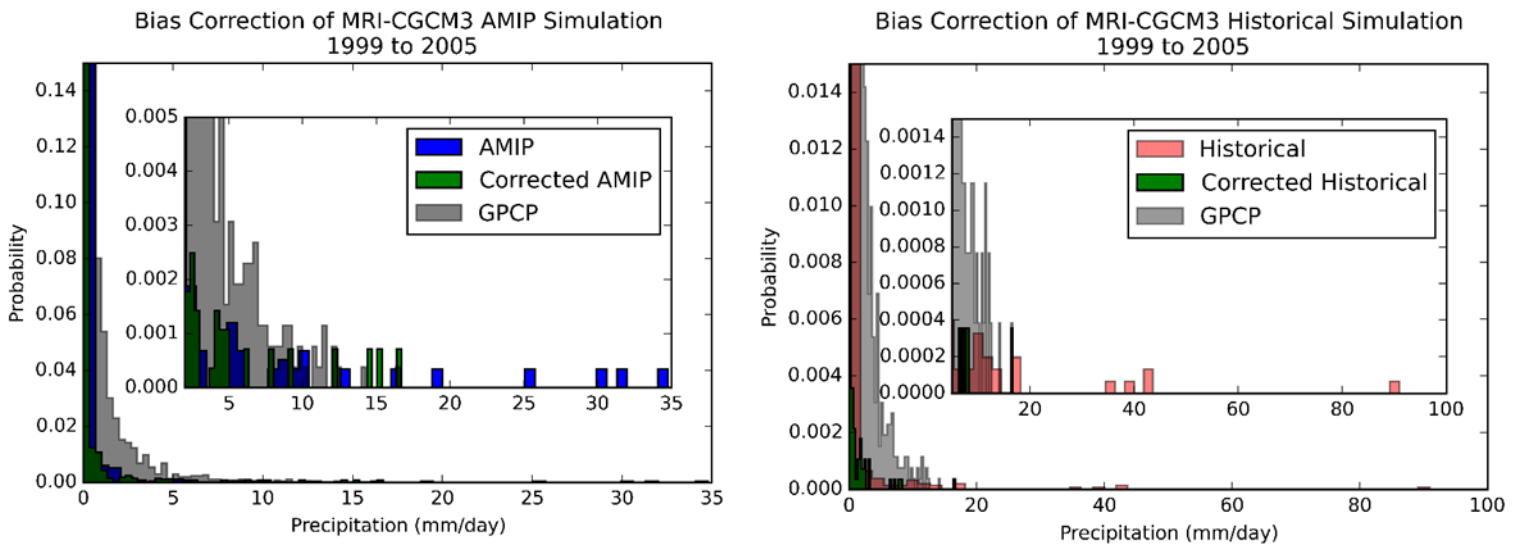
Figure 24: Quantile mapping used as a bias correction method to improve the performance of six CMIP5 model simulations, in comparison with the GPCP data. The inset is a zoomed in representation of the extreme events that cannot be seen in the distribution.

Summary

This chapter evaluated the performance of six CMIP5 model simulations (AMIP and Historical) and how they represent precipitation extremes, in comparison to the observations for the period 1999-2005. The observations used as a reference for the comparison are the gridded data (GPCP), as it was justified that they can represent the station data. It was concluded that almost all models overestimate the precipitation extremes, as well as their probability of occurrence and their variability. The closest model to the observations that succeeded in representing the extremes was the Canadian model CanAM4 and CanESM2. The worst model that failed to represent the extremes was the MRI-CGCM3 that underestimated the probability and variability.

The second section of this chapter was about proposing a correction method to the model simulations to properly represent the extremes. After the attempt maybe to use three methods, only the empirical quantile method was finally considered as it gave better results. The bias correction method gave satisfactory results that tried to approach the observations. However, the probability shown by the histograms of the corrected result is underestimated, as well as the variability.

6 Climate Model Projections

The last chapter of the findings is about the changes expected in extreme rainfall events due to climate change. The first section presents the projection made for Oman for the period 2035-2065 and the historical baseline period 1979-2005. Six CMIP5 models are used considering the RCP4.5 scenario. The second section of this chapter includes the bias correction of the climate model projections (CMP), using the gridded data (GPCP) as a reference and using the empirical quantile method. The third section presents the fixed thresholds above which each model considers extreme rainfall in the future. The threshold is then compared with the threshold resulted from the station data and the gridded data. The last section presents a spatial distribution of the precipitation changes expected in the future, using the mean relative changes.

6.1 General Future Projection in Oman

Six climate models are used to make future projections for precipitation in Oman during the period 2035-2065. A baseline period is used as well to show the change in the probability, as well as the shift of the histogram in the future. Three out of the six models shown in *Figure 25* agree that in general in Oman there will be an increase in precipitation as the histogram presented for the baseline period is shifting to the left. The probability of extreme events in the future is lower than in the historical period for most of the models. The HadGEM2, BCC-CSM1, and the MRI-CGCM3 are projecting days that may reach approximately 40 mm/day, 60 mm/day, and 235 mm/day respectively, higher than the baseline period 1979-2005.

On the contrary, the rest of the models project an overall decrease in precipitation in Oman. To be more specific, the GISS, CNRM-CM5, and Can-ESM2 are projecting days that may reach approximately 50 mm/day, 55 mm/day, and 5 mm/day respectively, lower than the baseline period 1979-2005. A probability of 0.0001 is equivalent to a single occurrence (1 day in the 30-year projection period).

HadGEM2 Historical Daily Precipitation
1979 to 2005
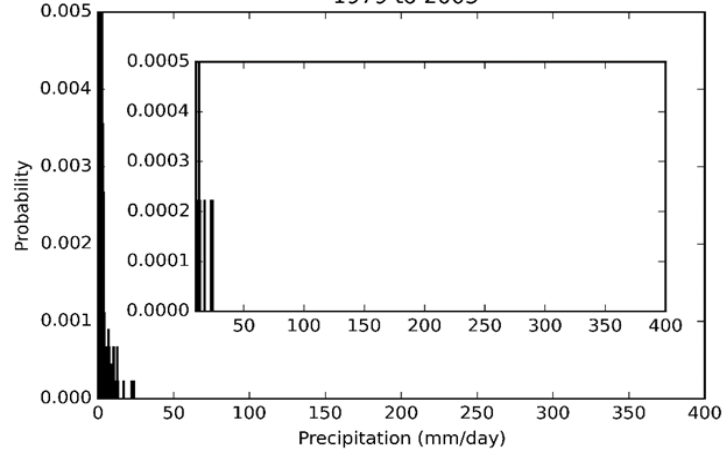
HadGEM2 Projection Daily Precipitation (RCP4.5)
2035 to 2065
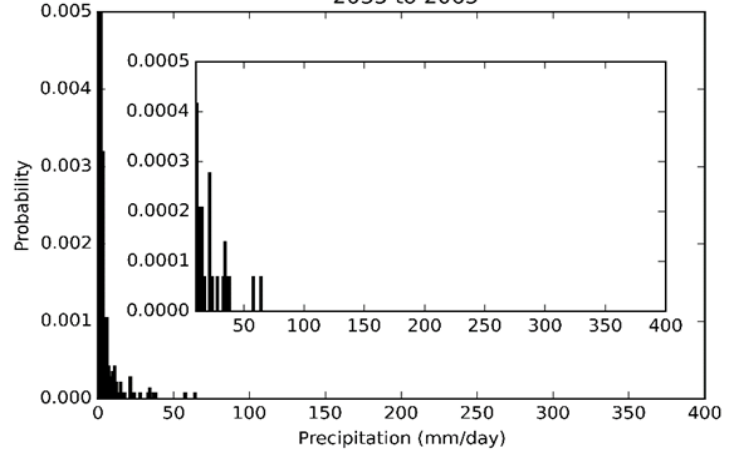
Can-ESM2 Historical Daily Precipitation
1979 to 2005
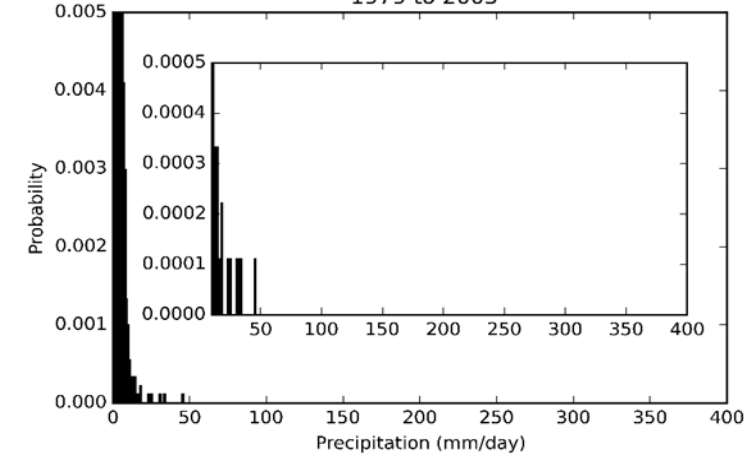
Can-ESM2 Projection Daily Precipitation (RCP4.5)
2035 to 2065
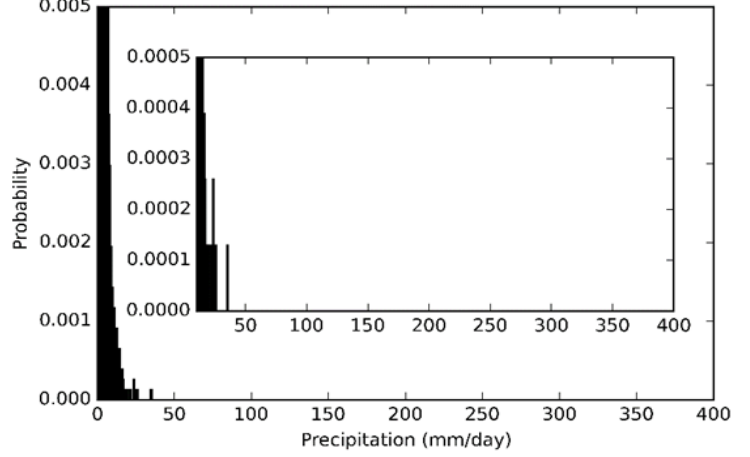
GISS Historical Daily Precipitation
1979 to 2005
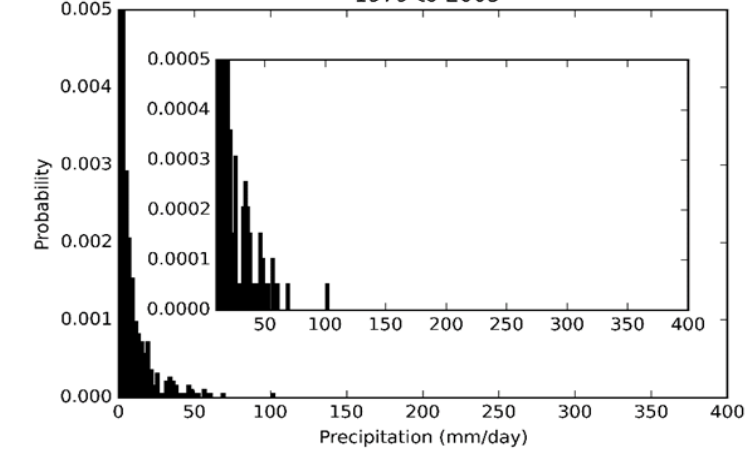
GISS Projection Daily Precipitation (RCP4.5)
2035 to 2065

47
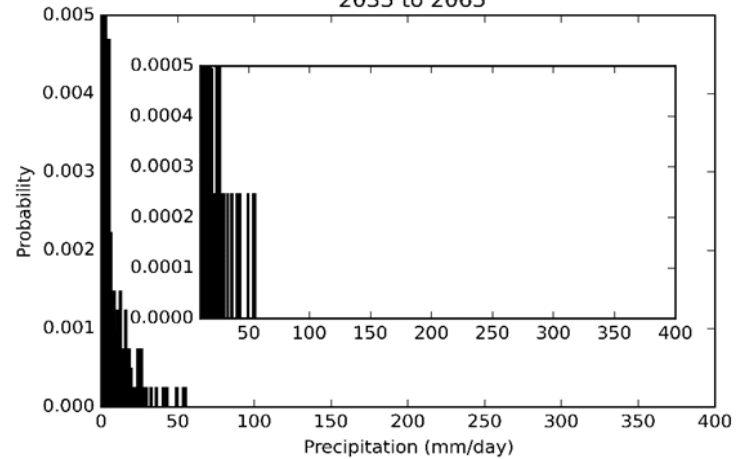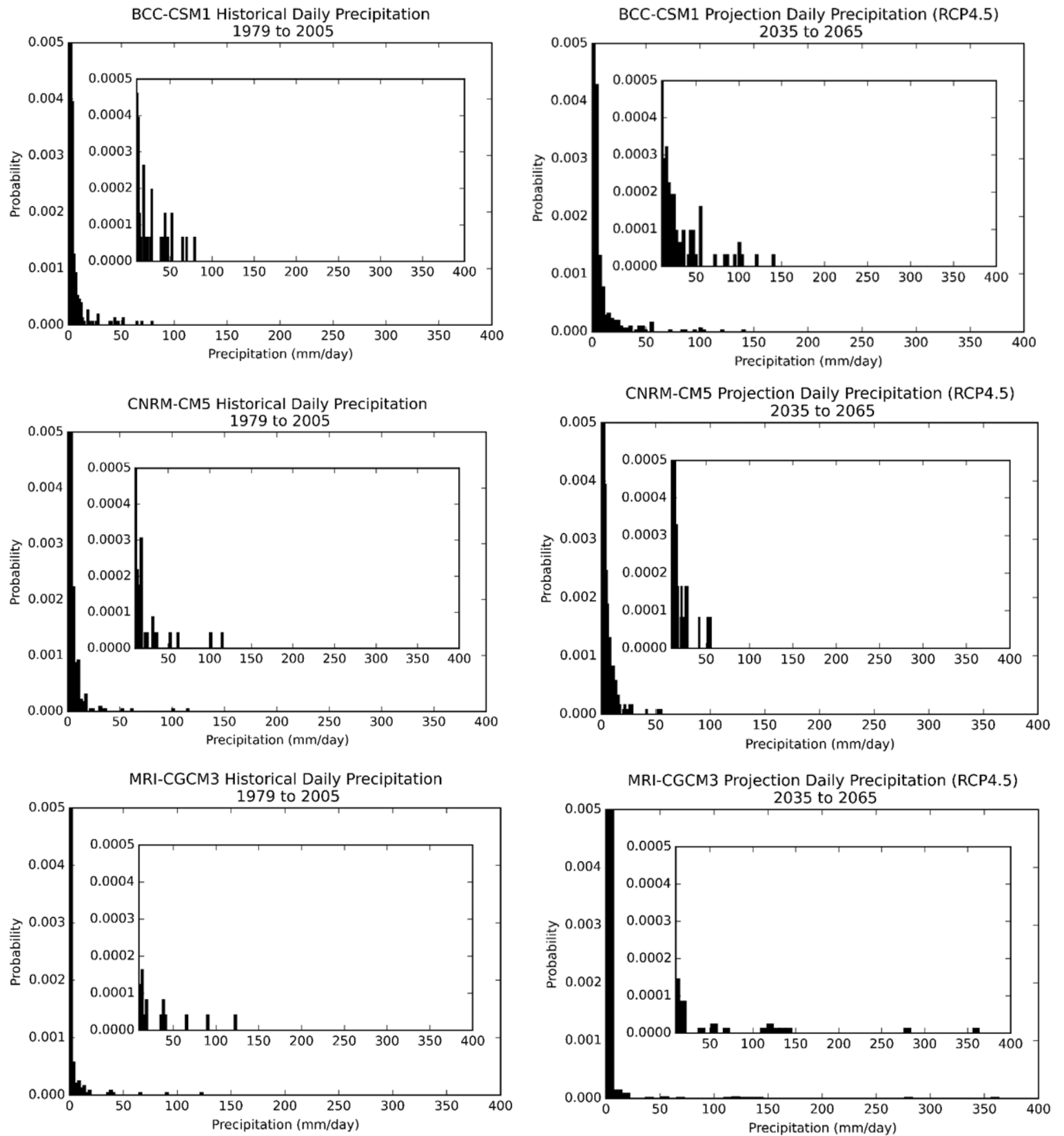
Figure 25: Histograms representing the future climate change projection for the period 2035-2065, and a baseline period 1979-2005. The models used are the CMIP5 models for the scenario RCP4.5.

6.2 Bias Correction of Climate Model Projections

This section uses the same bias correction method used in chapter 5, to propose a correction for the six future projection models. The correction is made based on the GPCP data that was used as well in correcting the AMIP and historical model simulations in chapter 5. The GPCP data period used in this chapter is 1996-2018. *Figure 26* illustrates the correction of the projections using the empirical quantile method. The corrected projections made for all models follow the same pattern in the histograms as the observations. However, as discussed previously in chapter 5, the correction made overall underestimates the probability of rainfall in comparison to the models and the observations.
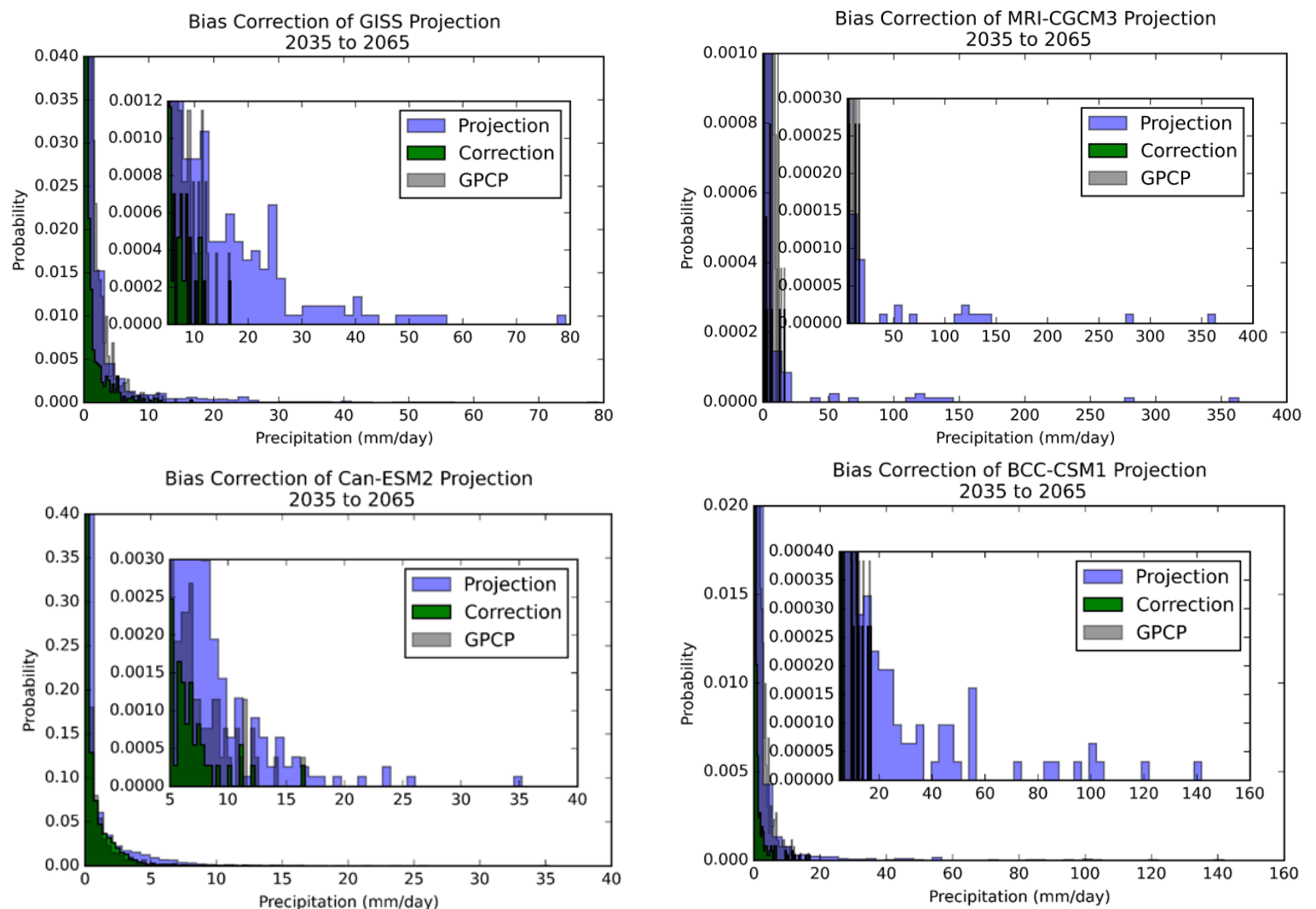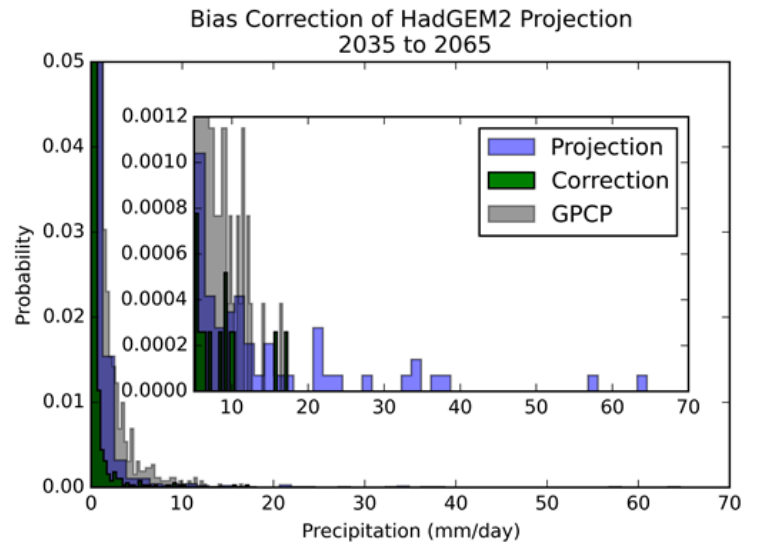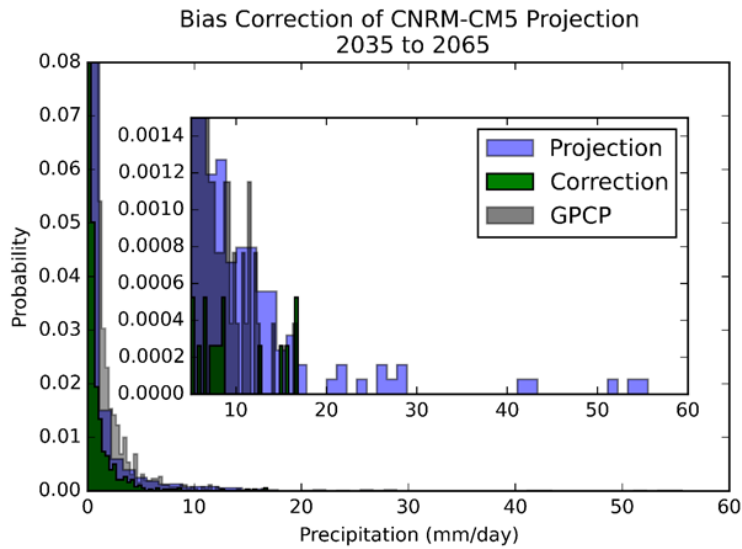
Figure 26: Quantile mapping used as a bias correction method to improve the performance of six CMIP5 model projections, in comparison with the GPCP data. The inset is a zoomed in representation of the extreme events that cannot be seen in the distribution.

6.3 Extremes Above a Fixed Threshold

This section proposes five fixed thresholds for each model separately, above which the models project extreme rainfall events. The thresholds are chosen using the results from *Figure 25*, as well as taking into consideration the thresholds chosen for the observations. The aim of this section is to examine whether the models correspond to the same threshold as the observations or not. In addition to that, the benefit is to check whether researchers and policymakers can rely on models to predict extreme rainfall events in Oman.
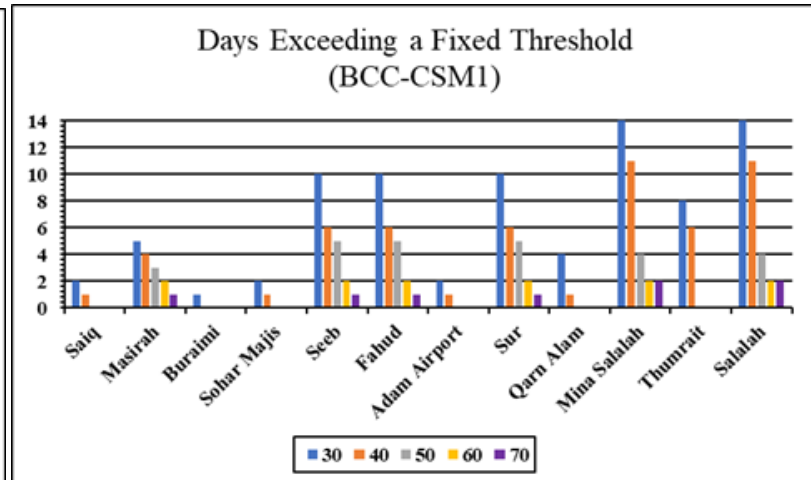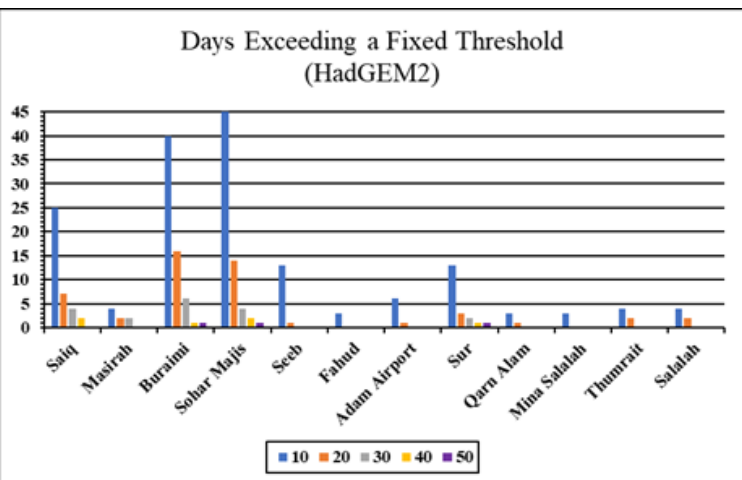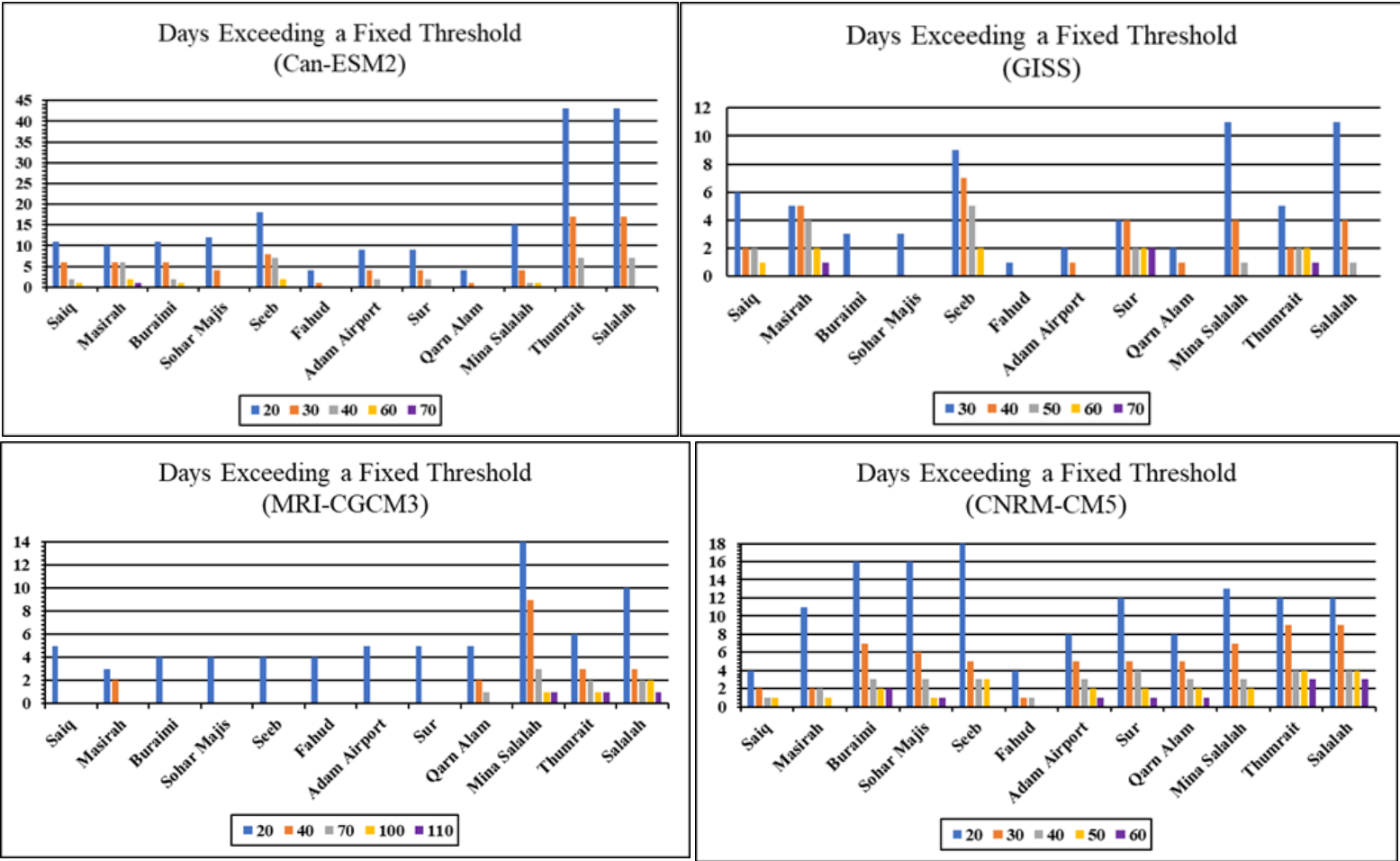
Figure 27: The graphs illustrate the days exceeding five fixed thresholds for each model projection in grid points that correspond to the 12 weather stations used in this study. The thresholds are an estimation of the extreme events that may be associated with flooding events in the future.

Figure 27 includes graphs that demonstrate the days exceeding five thresholds chosen for each model projections in grid points that correspond to the 12 weather stations used in this study. As mentioned in chapter 4, a fixed threshold above which Oman considers an extreme event is 50 mm/day, according to station data. It was also shown that for the gridded data, the extreme events in Oman are considered above 20 mm/day. The thresholds for the model projections are slightly different from each other, as each model projects the future extremes differently. Hence, it was found that for three out of the six models, an extreme rainfall event is above 20 mm/day. There is a slight difference in the maximum threshold of these three models, as well as the number of days exceeding that threshold, as they represent the future extremes in a different intensity (see *Figure 25*). The 20 mm/day threshold is like the GPCP threshold shown in *Figure 7*. The GISS model and BCC-CSM1, have a slightly higher threshold which is 30 mm/day, which is still closer to the gridded data than the station data. The only model with the

lowest threshold is the HadGEM2, that considers extreme rainfall event in Oman, rainfall above 10 mm/day, which is slightly closer to the gridded data threshold than the observations.

Having a closer look at the pattern given by the days exceeding the thresholds for each grid point that represents the location of stations, an estimation can be done on what to expect in different regions of Oman. In comparison to *Figure 7*, most of the models show an increase in the days of extreme rainfall in stations located in southern Oman, a high drop in daily extremes in northern Oman, and a slight decrease in the interior region which is mainly a desert. The HadGEM2 model and the CNRM-CM5, do not agree with the pattern represented by the rest of the four models, which will later be shown in the following section, that indeed the rest of the models gave the best estimations in terms of the expected intensity and rainfall distribution in Oman.

6.4 Future Climate

This last section is examining the changes between the past and the future spatial distribution of rainfall in Oman. The mean relative precipitation changes between the two periods (2035-2065 minus 1979-2005) and plotted. The plots are separated into three periods: annual changes, summer changes, and winter changes. The summer period in Oman starts from June and ends in September, and the winter period starts in November and ends in April, as already mentioned in chapter 2.
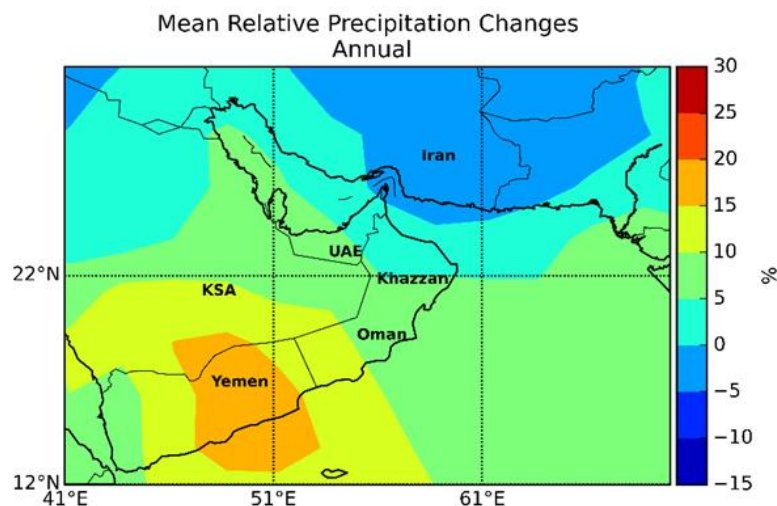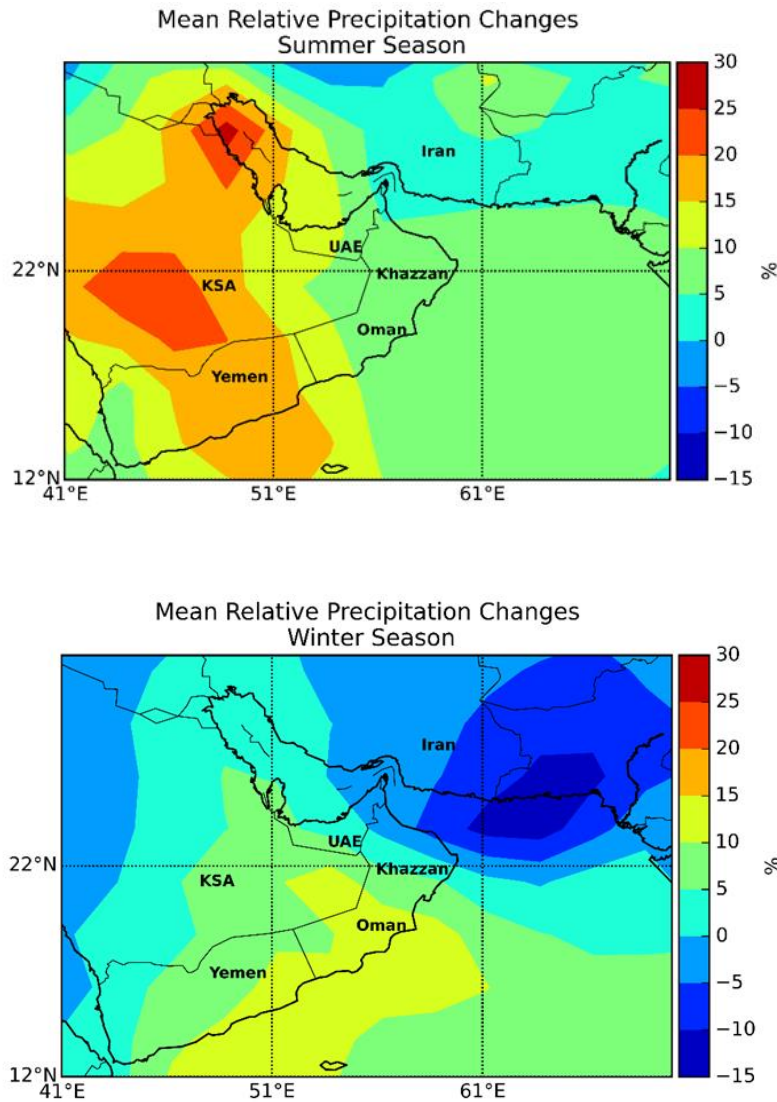
Figure 28: Mean RCP4.5 relative precipitation 2035-2065 minus 1979-2005 for three periods: annual, summer, and winter, using AR5 CMIP5 subset.

For precipitation it is better to plot the changes relative to the model climatology, than the absolute values. The hypothesis is that if the model has a strong bias in the mean it will have similar bias in the climate change signal and the relative change is then a better illustration of the signal than the absolute numbers. The relative changes are plotted in percentages.

Figure 28 shows the mean relative precipitation 2035-2065 minus 1979-2005 for three periods. From the three maps, it is evident that the northern part of Oman near Iran is getting drier with time, and it is going to be the driest part of Oman. During the summer season, the majority of Oman will show a mean relative change of 5-10%, while northern parts of Oman will show a change of rainfall around 0-5%. Southern Oman is expected to show an increase in the mean

relative precipitation change that ranges between 10-15%. During the winter season, almost half of Oman in the southern part is expected to show an increase in the mean relative precipitation change, that ranges between 10-15%. The northern part of Oman will be drier in all three periods, the southern part is expected to receive higher rainfall, and the interior region will show a neutral change. The general pattern followed, is drier conditions in northern Oman and gradual increase in the mean relative precipitation towards the south, which is different than the present distribution of rainfall in Oman (*Figure 2*).

Summary

The main highlights of this chapter are that half of the models used are projecting an increase in the daily rainfall in Oman, and the other half is projecting a decrease. The HadGEM2, BCC-CSM1, and the MRI-CGCM3 are projecting days that might reach approximately 40 mm/day, 60 mm/day, and 235 mm/day respectively, higher than the baseline period 1979-2005. On the contrary the GISS, CNRM-CM5, and Can-ESM2 are projecting days that may reach approximately 50 mm/day, 55 mm/day, and 5 mm/day respectively, lower than the baseline period 1979-2005. The empirical quantile method was then used as a bias correction method for the model projections, in comparison to the gridded GPCP data. A fixed threshold was then picked for each model that represents the extreme events and was compared with the threshold of the observations. Overall the thresholds were the same or close to the threshold for gridded GPCP data. The HadGEM2 model represents an extreme event above 10 mm/day, for the Can-ESM2, MRI-CGCM3 and CNRM-CM5 it is 20 mm/day, while for GISS and BCC-CSM1 it is 30 mm/day.

To have a clear image of the spatial distribution of the rainfall change in the future, the mean relative precipitation change was calculated in percentage. The maps showed that for the three periods the mean relative precipitation change indicates a drier environment in the future for northern Oman and a wet environment in the south. The same results were found by Al Charaabi et al. (2013) who used annual data.

7 Conclusions

The occurrence of extreme rainfall events and flash floods in many areas during recent years is a motivation to study long-term changes in extreme rainfall over Oman. The risk from the possible impacts of climate change has been growing with the recent cyclones that had affected the country. Gas and oil companies like British Petroleum (BP) require a deep knowledge about the past, the present climate and require an accurate estimation of the plausible change in extreme rainfall events. The study reveals the noticeable changes in the extreme rainfall events that occurred over Oman in the recent period.

There is an agreement between the station data and gridded data regarding the spatial distribution of extreme rainfall in Oman. The days exceeding a fixed threshold for both station data and the equivalent for gridded data was then calculated, to check which amount of daily rainfall is associated with extreme rainfall events and possible flooding. The lowest threshold considered for station data is 50 mm/day and 20 mm/day for gridded, and the highest threshold is 200 mm/day and 60 mm/day for the station data and gridded data respectively. It was concluded that gridded data do represent some daily extreme events, but they usually underestimate the magnitude of these events.

Almost all model simulations (AMIP and Historical) overestimate the precipitation extremes, as well as their probability of occurrence and their variability. The closest model to the observations that succeeded in representing the extremes was the Canadian model CanAM4 and CanESM2. The worst model that failed to represent the extremes was the MRI-CGCM3 that underestimated the probability and variability. After the attempt maybe to use three bias correction methods, only the empirical quantile method was finally considered as it gave better results. The bias correction method gave satisfactory results that tried to approach the observations. However, the probability shown by the histograms of the corrected result is underestimated, as well as the variability.

The HadGEM2, BCC-CSM1, and the MRI-CGCM3 are projecting days that might reach approximately 40 mm/day, 60 mm/day, and 235 mm/day respectively, higher than the baseline period 1979-2005. On the contrary the GISS, CNRM-CM5, and Can-ESM2 are projecting days that may reach approximately 50 mm/day, 55 mm/day, and 5 mm/day respectively, lower than the baseline period 1979-2005. A fixed threshold was then picked for each model that represents the extreme events and was compared with the threshold of the observations. Overall the thresholds were the same or close to the threshold for gridded GPCP data. The HadGEM2

model represents an extreme event above 10 mm/day, for the Can-ESM2, MRI-CGCM3 and CNRM-CM5 it is 20 mm/day, while for GISS and BCC-CSM1 it is 30 mm/day. The maps showed that for the three periods the mean relative precipitation change indicates a drier environment in the future for northern Oman and a wet environment in the south.

Future researchers, industries, and policy makers can rely on model projections; however, a combination of station data, gridded data and models would be the best to have a clear image and reduce uncertainties.

8 Bibliography

Al-Awadhi, T., Y. Charabi, B. S. Choudri, and Y. Bani Oraba, 2018: Flooding risk analysis: A case study of Muscat Governorate, Sultanate of Oman, *Hum Ecol Risk Assess*, **24**, 667-678, doi: 10.1080/10807039.2017.1396441.

Alexander, L. V., and Coauthors, 2006: Global observed changes in daily climate extremes of temperature and precipitation. *J Geophys Res*, **111**, 1-22, doi: 10.1029/2005JD006290.

Al-Hatrushi S. M. 2012: Rainfall variability & its impact on water resources in Oman, Conference paper.

Al-Kalbani, M. S., and J. C. Martin, 20015: Recent Trends in Temperature and Precipitation in Al Jabal Al Akhdar, Sultanate of Oman, and the Implications for Future Climate Change, J *Earth Sci Clim Change*, **6**, 295, doi: 10.4172/2157-7617.1000295.

Allen, M. R., and W. J. Ingram 2002: Constraints on future changes in climate and the hydrologic cycle. *Nat,* **419**, 224-232.

Al-Rawas, G. A. 2009: *Flash Flood Modelling in Oman Wadis. A Thesis submitted to the faculty of graduate studies in partial fulfilment of the requirements for the degree of Doctor of Philosophy*, Calgary University, Calgary, AB, Canada.

Al-Rawas, G. A. 2010: Relation between Wadi drainage characteristics and peak flood flows in arid northern Oman, *Hydrol Sci J*, **55**, 377-393.

Al-Sharmi, S. and R. Washington, 2011: Recent observed climate change over the Arabian Peninsula. *J Geophys Res,* **116**.

Abarbane, H., S. Koonin, H. Levine, G. MacDonald, O. Rothaus, 1992: Statistics of Extreme Events with Application to Climate.

Balsamo, G., and Coauthors, 2015: ERA-Interim/Land: a global land surface reanalysis data set, *Hydrol Earth Sys Sci*, **19**, 389, doi: 10.5194/hess-19-389-2015.

Ban, N. Schmidli, J. and C. Schar, 2015: Heavy Precipitation in a changing climate: Does short-term summer precipitation increase faster? *Geophys Res Lett*, **42**, 1165-1172, doi: 10.1002/2014GL062588.

Beniston, M., and Coauthors, 2007: Future extreme events in European climate: an exploration of regional climate model projections, *Clim Change*, **81**, 71-95.

Bp.com. 2016: BP's Khazzan gas project in Oman nears completion of phase one, Accessed 8 July, 2018, https://www.bp.com/en/global/corporate/media/press-releases/bps-khazzan-gas-project-in-oman-nears-completion-of-phase-one.html

Cannon, A. J., S. R. Sobie, and T. Q. Murdock, 2015: Bias Correction of GCM Precipitation by Quantile Mapping: How Welll Do Methods preserve Changes in Quantiles and Extremes? *Am Meteorol Soc*, **28**, 6938-6959, doi: 10.1175/JCLI-D-14-00754.1.

Charabi, Y. S. Al-Hatrushi, 2010: Synoptic aspects of the winter rainfall variability in Oman. *Atmos Res,* **95**, 470-486.

Charabi, Y. and S. Al-Yahyai, 2013: Projection of Future Changes in Rainfall and Temperature Patterns in Oman. *J Earth Sci Clim Change*, **4**.

Confluence.ecmwf.int. 2018: What is ERA-Interim - Copernicus Knowledge Base - ECMWF Confluence Wiki. Accessed 1 August 2018, https://confluence.ecmwf.int//display/CKB/What+is+ERA-Interim

Data, C. 2009: Guidelines on analysis of extremes in a changing climate in support of informed decisions for adaptation. World Meteorological Organization.

 Dee, D. P., and Coauthors, 2011: The ERA-Interim reanalysis: configuration and performance of the data assimilation system, *Q J Roy Meteorol Soc*, **137**, 553– 597, doi:10.1002/qj.828.

Fisher, M. 1994: Another Look at the Variability of Desert Climates, Using Examples from Oman. *Global Ecol Biogeography Lett*, **4**, 79-87.

Fowler, H. J., and Coauthors, 2005: New estimates of future changes in extreme rainfall across the UK using regional climate model integrations, 1. Assessment of control climate. *J Hydrol*, **300**, 212-233.

Goswami, B. N., V. Venugopal, D. Sengupta, M. S. Madhusoodanan, and P. K. Xavier, 2006: Increasing trend of extreme rain events over India in a warming environment; *Sci,* **314**, 1442-1445.

Guhathakurta, P., O. Sreejith, and P. Menon, 2011: Impact of climate change on extreme rainfall events and flood risk in India. *J Earth Syst Sci*, **120**, pp.359-373.

Gunawardhana, L. N., and G. A. Al-Rawas, 2014: Trends in extreme temperature and precipitation in Muscat, Oman. *Proc Int Assoc Hydrol Sci,* **364**, 57-63.

Gunawardhana, L. N., G. A. Al-Rawas, S. Kazama, and K. A. Al-Najar, 2015: Assessment of future variability in extreme precipitation and the potential effects on the wadi flow regime, *Environ Monit Assess* **187**, doi: 10.1007/s10661-015-4851-5.

Gutjahr, O. and G. Heinemann, 2013: Comparing precipitation bias correction methods for high-resolution regional climate simulations using COSMO-CLM. Effects on extreme values and climate change signal, *Theor Appl Climatol*, **114**, 511-529.

Haggag, M. and H. Badry, 2012: Hydro meteorological modelling study of Tropical Cyclone Phet in the Arabian Sea in 2010. *Atm Clim Sci*, **2**, 174– 190.

King, A. D., Alexander, L. V., and Donat, M. G. 2012: The efficacy of using gridded data to examine extreme rainfall characteristics: a case study for Australia, *Int J Climatol*, **33**, doi: 10.1002/joc.3588.

Kwarteng, A. Y., A. S. Dorvlo, T. K. Ganiga, 2008: Analysis of a 27-year rainfall data (1977-2003) in the Sultanate of Oman. *Int J Climatol,* **29**, 605-617.

Latlong.net. 2018: Muscat, Oman Map Lat Long Coordinates. Accessed 30 July 2018, https://www.latlong.net/place/muscat-oman-1035.html

Liu, C. and R. Allan, 2013: Observed and simulated precipitation responses in wet and dry regions 1850–2100, *Environ Res Lett*, **8**, 1-11.

Metoffice.gov.uk. 2018: Met Office: UKCP09 gridded observation data sets - frequently asked questions, Accessed 28 July, 2018, https://www.metoffice.gov.uk/climatechange/science/monitoring/ukcp09/faq.html

Ministry of Regional Municipalities, Environment and Water Resources MRMEWR, 2015: *Water resources management and development in Oman*, http://www.sesam-uae.com/muscat/presentations/Dr.%20Saif,%20Ministry%20of%20Regional%20Municipalities%20and%20WR.pdf

Ncdc.noaa.gov. 2018: National Centers for Environmental Information (NCEI) formerly known as National Climatic Data Center (NCDC) | NCEI offers access to the most significant archives of oceanic, atmospheric, geophysical and coastal data, Accessed 1 August, 2018, https://www.ncdc.noaa.gov/

O'Gorman, P. A., and T. Schneider 2008: The hydrological cycle over a wide range of climates simulated with an idealized GCM, *J Clim*, **21**, 3815–3832, doi:10.1175/2007JCLI2065.1.

Pendergrass, A. G. 2018: What precipitation is extreme? *Sci*, **360**, 1072-1073, doi: 101126/science. aat1871.

Piani, C., J. O. Haerter, and E. Coppola, 2010: Statistical bias correction for daily precipitation in regional climate models over Europe, *Theor Appl Climatol*, **99**, 187-192.

Pianka, E. R. 1970: On r- and K-selection. *Am Nat*, **104**, 592-597.

Schoonjans, F., D. De Bacquer, P. Schmid, 2011: Estimation of population percentiles, *Epidemiology*. **22**, 750–751, doi:10.1097/EDE.0b013e318225c1de.

Slobodkin, L. B. and H. L. Sanders, 1969: On the contribution of environmental predictability to species diversity. *Brook Symp Biol*, **51**, 82-95.

Stirzaker, D. 2007: *Elementary probability*. Cambridge University Press.

Thomson, A. M., and Coauthors, 2011: RCP4.5: a pathway for stabilization of radiative forcing by 2100, *Clim Change*, **109**, 77–94.

Times of Oman, 2018: Salalah gets over 5 years of Oman's average annual rain. Accessed 9 July 2018, https://timesofoman.com/article/135263

Yekambessoun, N. M., E. L. Agnide, T. O. Ganiyu, K. Y. Benjamin, A. A. Abel, 2016: Camparison of Daily Precipitation Bias Correction Methods Based on Four Regional Climate Model Outputs in Oueme Basin, Benin. *Hydrol*, **4**, 58-71, doi: 10.11648/j.hyd.20160406.11.